

INTERIM
IN-24-CR

**EFFECT OF IMPACT DAMAGE
AND OPEN HOLE ON COMPRESSIVE STRENGTH
OF HYBRID COMPOSITE LAMINATES**

by

**Dr. Clem Hiel, Research Scientist
Division of Engineering
The University of Texas at San Antonio
San Antonio, TX 78249**

(NASA-CR-194603) EFFECT OF IMPACT
DAMAGE AND OPEN HOLE ON COMPRESSIVE
STRENGTH OF HYBRID COMPOSITE
LAMINATES Final Report, 1 Jun. 1992
- 31 May 1993 (Texas Univ.) 77 p

N94-16836
--THRU--
N94-16837
Unclas

G3/24 0191357

**Prepared for NASA Cooperative Agreement NCC2-724
Period: June 1, 1992 - May 31, 1993**

CONTENTS

I Effect of Impact Damage and Open Hole on Compressive Strength of Hybrid Composite Laminates

II Appendix: Papers published during grant period June 1, 1992- May 31, 1993

- Low and High Velocity Impact Response of Thick Hybrid Composites
Proceedings of the American Society for Composites,
Seventh Technical Conference, pp 1149-1159, Oct 1992**
- Damage Tolerance of a Composite Sandwich with Interleaved Foam Core.
Journal of Composites Technology & Research,
Fall 1992, pp 155-168**
- Composite Sandwich Construction with Syntactic foam Core.
Composites, Volume 24. Number 5, 1993, pp 447-450**

6 October, 1993

Effect of Impact Damage and Open Hole on Compressive Strength of Hybrid Composite Laminates

Clement Hiel¹

NASA Ames Research Center, Moffett Field, California, 94035

Abstract

Impact damage tolerance is a frequently listed design requirement for composites hardware. The effect of impact damage and open hole size on laminate compressive strength was studied on sandwich beam specimens which combine CFRP(*)-GFRP(**) hybrid skins and a syntactic foam core. Three test specimen configurations have been investigated for this study. The first two were sandwich beams which were loaded in pure bending (by four point flexure). One series had a skin damaged by impact, and the second series had a circular hole machined through one of the skins. The reduction of compressive strength with increasing damage (hole) size was compared. Additionally a third series of uniaxially loaded open hole compression coupons were tested to generate baseline data for comparison with both series of sandwich beams.

(*) CFRP : Carbon Fiber Reinforced Plastic

(**) GFRP : Glass Fiber Reinforced Plastic

¹ Research Scientists, NASA cooperative Agreement NCC 2-724 with Division of Engineering at the University of Texas at San Antonio. (Prof. H.F. Brinson Principal Investigator)

It was concluded that post-impact strength of sandwich skins can be predicted by using an open hole analytical model in which the observed (measured) damage size is used as input.

The results reveal the same dependency of strength on-damage size (or hole size) for both sandwich beam series. This can be attributed to the local nature of the impact damage within the skin. Such damage is typically observed in sandwich beams with syntactic foam core. The baseline data for sandwich skin coupons indicates lower strength as compared to sandwich data for the same hole size.

The use of an empirical-analytical procedure to predict the residual strength of impacted sandwich beams, based on open hole skin laminate analysis and test data for uniaxial loading, leads to conservative strength predictions. The higher post-impact performance of sandwich beam skins, as compared to skin coupons, is attributable to the lateral skin support provided by the structural syntactic foam which prevents global- and micro buckling induced-failure modes.

INTRODUCTION

Impact damage tolerance is a frequently listed design requirement for composites hardware. The success of composite materials applications in secondary loaded structures, combined with its potential for primary structures has spurred intensive research programs aimed at integrating materials into hybrid-, damage tolerant-structural configurations.

It can be generally stated that the damage tolerance of structural composite materials is low, in comparison to (homogeneous) metals. Especially composites with thermoset matrix are sensitive to stress concentrations due to surface cuts, notches, holes, impact damage and other material or geometric discontinuities which promotes crack-initiation and -propagation. Unlike to homogeneous materials, fiber reinforced composites are significantly more notch sensitive in compression than in tension. This is due to the development of tensile stresses which are, in the vicinity of a notch or free edge, acting perpendicular to the fibers and to the lamina. Another major reason is the formation of

delamination due to impact, which enhances sublaminar buckling mechanisms under compressive loading. Most of the research work aimed at ranking different composite materials, based on their damage tolerance performance has been motivated by CAI ("Compression After Impact" type of testing

The effect of lateral impact on composite laminates can as a first approximation be looked at as a hole (only when damage is localized). Early studies on the effects of holes and other geometric discontinuities in composites have been based on Lekhnitski's classical analytical solution for the stress distribution in anisotropic plates [1,2]. Follow-up studies have concentrated on the effect of hole size on the strength of laminated composites under uniaxial tension and compression [3,4].

Numerous analytical and empirical studies have dealt with parametric effects, such as stacking sequence or material composition on compressive strength and stability of open hole specimens [5-12]. These investigations have been motivated by two major objectives: The first was to provide a database and analytical models for design and prediction of the mechanical performance of bolted (or pinned) composite joints. The mechanical behavior of fastened composite joints was investigated extensively during the last decade [13-17]. The information available to date on bearing stresses at the hole contour as well as stress distribution in the vicinity of the hole provides the data required for strength assessment and optimized composite joint design [18]. The second objective was to assess the effect of damage (mainly due to lateral impact) on the residual compressive strength of structural composite elements. Attempts to use the open hole model to predict impact damage effects on composite residual strength, on the other hand, were not so successful [19-21]. This is mainly due to the highly complicated geometric pattern, and the mixed multiple failure mode characteristics which are typical for impact damage in most composite material laminates [22-26]. Multiple delaminations of different shapes and sizes are dispersed

randomly throughout the laminate width and thickness. This is combined with extensive matrix- and inter-fiber cracks and with fiber fractures. Furthermore, the compressive strength of impact damaged laminates is mainly controlled by a sublaminar buckling mechanism [27-30]. Such failure characteristics could hardly be represented by the simple and well defined open hole geometry. Similar comments may be relevant for the case of impact damaged composite sandwich panels with honeycomb cores [31-33].

This report provides additional information on the damage tolerance and residual strength prediction of a new structural configuration which was developed by the authors [34,35]. This composite sandwich system utilizes a syntactic foam core which has considerably more strength and stiffness as compared to the common polymeric foams. This system is able to sustain significant flexural loading as compared to thin laminates which are designed solely for in-plane loading. Additionally the performance of composite sandwich panels with syntactic foam core has been proposed as the basic building block for a composite compressor blade [35,36]. It was shown that in such sandwich construction, damage is locally confined within a well defined boundary and may therefore be treated like an open hole. This is attributed to the local energy absorption capacity provided by the syntactic foam core [37]. This applied composites technology program has had so much bite that it has drawn interest from across the general consumer product sector.

Three different test configurations have been compared in this report. The first two were sandwich beams which were loaded in pure bending (four point flexure). For one series the skin was damaged by impact, and for the second, a circular hole was carefully machined through one of the skins. The reduction of compressive strength with increasing damage (hole) size was compared. Additionally a third series of uniaxially loaded open hole compression coupons were tested to generate baseline data for comparison with both series of sandwich beams.

The three main objectives of the present research were:

1. Experimentally verify the applicability of an open hole model for the prediction of residual strength after impact.
2. Compare the compressive strength of laminate sandwich skins with open holes by loading a sandwich beam in pure flexure with the compressive strength of uniaxially loaded skin coupons.
3. Develop an empirical-analytical procedure which can be utilized to predict the residual strength of impact damaged sandwich beams under flexure, based on a simple open hole skin laminate analysis and test data for uniaxial loading.

The information in this report has been organized in four sections. The first describes the basic materials used to build the test samples, and their material properties. The second section details the three test configurations, which were compared in this study, and the associated test procedures. The third section gives the test results and organizes the obtained experimental results for interpretation. Additionally, an empirical-analytical model is discussed which can be utilized for predictive purposes. The fourth and last section lists three conclusions which are supported by this research.

MATERIALS AND PROPERTIES

The structural configuration, proposed by the authors, is shown in Figure 1. These sandwich beams were cut from larger panels to a length of 355 mm (14") and a width of 76 mm (3"). The overall thickness is about 34 mm (1.34"). As indicated in Figure 1, the sandwich beam consists of five different basic materials for which more details and properties are given below.

Materials

The **Core (1)** for the sandwich specimens was made of precast syntactic foam (SYNTAC 350) supplied by Grace Syntactic Company. It consists of epoxy resin filled with glass micro balloons having the average density of 0.6 gr./cm³.

The skin laminate consists of a central **Carbon Fiber Reinforced (CFRP) laminate (2)**, layers of glass weave on both sides of the skin, and **film adhesive (3)** to intimately bond the glass weave to the center laminate. The central CFRP laminate, was fabricated from unidirectional carbon fiber reinforced Bismaleimide prepreg tapes (rigidite G40-600/5245C) supplied by BASF. It consists of 18 plies, with .14 mm (.005") average ply thickness, and with a (0/+30/-30)_{3s} lay-up. Two layers of **glass fabric reinforced epoxy (GFRP) (4)** prepregs (7781/ 5245C) were placed above and below the CFRP laminate for external protection of the skin. Two layers of FM300 prepreg adhesive film (made by American Cyanamid corp.) were placed between the CFRP laminate and the GFRP.

The skin laminate, with a total of 22 plies, was cured at 177°C (350°F) in a press with heated platens, following the so called "standard 350 F cure cycle" as supplied by the prepreg manufacturer. The measured average thickness of the cured skin laminate was 2.52 mm (.099").

The adhesive used to bond the skins to the core was a Hysol EA9394 **room temperature curable adhesive (5)**. The sandwich beam obtained, as shown in Figure 1 has also been referred to by the authors as a "**Thick Hybrid Composite**" (THC).

Material Properties

The basic material properties of the cured, unidirectional CFRP lamina, the GFRP fabric, the syntactic foam, and the adhesive layers are given in Table 1. They are designated for the cured state at room temperature (RT.) dry condition. Most of the constituents' data was obtained from the available literature and supplier information. The properties of the syntactic foam were obtained independently following ASTM test standards (D638 for tensile properties, C365 for

compressive strength and C273 for shear properties). Most of the CFRP skin properties were computed based on the respective lamina inputs, using composite laminate analysis, except for the compressive strength (F_{ic}) and the coefficients of thermal expansion (α_1, α_2) which were obtained experimentally.

TEST CONFIGURATIONS AND PROCEDURES

Figure 2 gives an overview of the three test configurations, which were used for this study. This section contains a description and the test procedure for all three configurations.

Series 1: Impact damaged sandwich skin laminates; The upper skin of a sandwich beam flexural test configuration, which was shown in Figure 1 and discussed above, was impacted by using a low velocity (drop weight) instrumented impact system. After the impact, there remains a visible indentation with a diameter D which depends on the impact energy. The impact test machine has a maximum drop height of 3 meters (9.8 feet) and is commercially known as the Impac 66 test machine made by Monterey Research Laboratories. The impactor is a 16 mm (.625") diameter hemispherical (hardened steel) tip attached to a rigid base with the assembly weighing 86N. The impactor is raised to the required height by a chain winch which is driven by an electric motor. Two lubricated circular columns guide the impactor during its fall. Subsequently the weight is released pneumatically and impacts the test-sample. The rebound of the impactor is arrested automatically by a braking system to insure a single impact event. The values of the impact variables were defined experimentally to account for the friction during falling. The velocity was determined by measurement of the elapsed time between two photo cells. The actual maximum kinetic impact energy just before the collision was calculated from this velocity. The average calculated drop acceleration was about 0.88g. The dynamic response of the system during the impact process was monitored by an H.P. Dynamic Signal Analyzer (type 3562A) An Endevco type 2252 accelerometer was attached to the

top of the impactor. The impacted sandwich beam specimens were simply supported on two rollers having a span of about 200 mm (8") as indicated in Figure 3.

After impact the visible damage size along the beam width and the damage depth were measured. Subsequently the damaged sandwich beams were loaded to failure in a 4-point flexure set-up as illustrated in Figure 4. The loading configuration puts the side with the damaged skin in compression. A constant cross-head speed of 1.84 mm/min (.07"/min) was maintained during this test.

Series 2: Open hole sandwich skin laminates; were obtained by pre drilling one of the skins in the sandwich beam configuration (Figure 1) before bonding it onto the core. Hole diameters in this case varied between 3.05 and 22.2 mm (.12" and .87").

The residual strength was obtained by using the four-point bend procedure, which now put the side with the hole in compression. The cross-head speed was the same as for series 1 (1.84 mm/min or .07"/min).

Series 3: Open hole skin coupon laminates; These coupons were obtained by utilizing only the skin laminate. The test procedure followed the SRM 3-88 (SACMA recommended method 3-88) which is detailed in reference [38]. The special SACMA SRM 3-88 compression fixture is shown in Figure. 5. The test method is based on NASA RP 1092 [39]. Specimen dimensions were 38.1 x 305 mm (1.5" x 12") and the hole diameters (D) varied from 1.5 to 11.1 mm (.06" to .44") as shown in Figure 5. Specimens without hole for determination of reference compressive strength data were prepared and tested according to SRM 1-88. The special test fixture is shown in Figure 6. The test method is based on ASTM D695. Respective dimensions were 12.7 x 80.8 mm (.5" x 3.18") as shown in Figure 14c. [40].

In both tests, specimens were loaded to failure in compression at constant cross head speed of 1.27 mm/min (.05"/min)

TEST RESULTS

Most of the test results deal with the effect of damage (or hole) size on laminate strength. Due to the complex and different hybrid compositions involved in the present investigation, strength data obtained for sandwich skin laminates (series 1 & 2) and for skin coupon laminates (series 3) could only be compared by referring to the maximum stresses at failure (σ_{cf-max}) acting on the same material phase (the CFRP laminate in this case). Stress distributions through the different phases of the skin coupon are shown in Figure 7. The stress σ_x shown on the left hand side is the average axial compressive stress which is obtained by dividing the load at failure by the cross-sectional area. The stress distribution shown on the right hand side in Figure 7 accounts for the stiffness contrast between the carbon phase and the glass phase. Therefore, as indicated, the stress in the carbon is α times higher than the average stress. A value for $\alpha = 1.45$ was obtained by laminate analysis. The stress level σ_{xcf} in the carbon phase at skin coupon failure is considered representative for the in-situ compressive strength of the CFRP laminate. Figure 8 shows the stress distribution in the sandwich skin laminate. Here the correction factor γ converts the maximum compressive stress $\bar{\sigma}_{cf}$ which is obtained from simplified sandwich analysis to a stress $\bar{\sigma}_{cf}$, which is the accurate maximum compressive stress on the carbon phase at skin failure. A value for $\gamma .882$ has been found for the basic sandwich configuration by substituting the dimensions specified in Figure 8 and the material properties found in Table-1 into a laminate analysis program.

The test results for all three configurations, which are reported below, give the stress in the carbon phase at skin failure. An interpretation of these results is given subsequently.

Series 1: Impact damaged sandwich skin laminates;

Impact damage characteristics: As was mentioned before, impact damage of a sandwich with syntactic foam core is local and well confined within a zone which is approximately circular. This zone can be inspected easily due to a damage induced indentation and a white imprint at the GFRP fabric coating as shown in Figure 9. The boundary of this imprint is a good representation of the internal non- visible CFRP damage zone beyond which the skin may be considered as non-damaged as can be seen by the cross sectional view of the local damage shown in Figures 10 and 11. Hence, the transverse measure of this imprint was defined as **damage size** to be compared to the open hole diameter in test configuration 2. The damage size seems to be directly related to the increase of the impact energy, as shown in Figures 11 and 12. Similar results were obtained in another study [35] for sandwich beams with interleaved syntactic foam core. Additionally this trend was also demonstrated for the case of sandwich beams subject to high velocity (ballistic) impact tests [36].

Effect of damage on residual strength : Nominal Compressive Strength was obtained from the flexural test results of impact damaged sandwich beams. Nominal Strength is defined here as the maximum skin stress per unit nominal cross-sectional area (disregarding the presence of damage) at sandwich failure. Increase of the damage size causes a pronounced deterioration effect on nominal strength for the small damage size range shown in Figure 13. For larger damage sizes this effect becomes less and less significant. Shear failure, originating from the damage boundary, following the fibers at the 30-deg angle was seen as the controlling failure mode. (Shown in Figure 14a). Similar results were also found in earlier studies for the case of sandwich beams subject to high velocity (ballistic) impact tests [41].

Series 2: Open hole sandwich skin laminates;

The relationship between Nominal Compressive Strength and hole diameter, shown in Figure 15, was obtained experimentally from four point flexure tests on open hole sandwich beams. The data was seen to follow a trend similar to that observed in Figure 13 for the post- impact sandwich specimens.

The observed failure mode, shown in Figure 14b, was also similar. It may therefore be concluded, at this stage, that damage size definition for the post-impact sandwich is justified and that the effect of impact damage on residual strength can be evaluated based on respective open hole sandwich data and analysis.

Series 3: Open hole skin coupon laminates;

The relationship between Nominal Compressive Strength and hole diameter, shown in Figure 16 was obtained experimentally from uniaxial compressive tests on open hole skin coupon specimens. The data follows a trend similar to that obtained for series #1 and #2 except that the strength degradation rate is higher, especially in the small hole diameter range. The observed failure mode, shown in Figure 14c was found to be similar to the one observed for series #1 and #2 sandwich beam specimens i.e, predominantly shear failure along 30-deg fiber orientation at the CFRP laminate. This failure mode is also similar to that for virgin specimens, which was shown earlier in Figure 6.

INTERPRETATION

A. Analytical background

The analytical formulations which were developed in references[2, 3 & 41] for the prediction of open hole compression strength will be used to examine the experimental results and to provide analytical tool for prediction of post-impact strength of sandwich beams based on damage size measurements. This is justified in light of the well defined

localized impact damage which was found to be typical for the sandwich having syntactic foam core in the present investigation. According to this model the compressive stress at failure, σ_N is a function of the hole diameter (D) and the specimen width (W) as shown in Figure 17.

As indicated in Equation 1, the notched strength (which is experimentally measurable) can be obtained by dividing the strength of an infinitely wide laminate by a correction function Y

$$\sigma_N = \frac{\sigma_N^\infty}{Y(D/W)} \quad (1)$$

The correction function can be calculated as follows

$$Y_{D/W} = \frac{2 + (1 - D/W)^3}{3(1 - \frac{D}{W})} \quad (2)$$

Strictly speaking this equation is only correct for isotropic laminates and therefore Y is called the "isotropic width correction factor". Gillespie et al [42] have shown nevertheless that the above expression is applicable to orthotropic laminates for D/W values smaller than .25, which was the case in this investigation.

According to Whitney and Nuismer [3] the notched strength of an infinitely wide orthotropic plate is related to the unnotched strength by the following equation;

$$\sigma_\infty^N = \frac{2\sigma_0(1-\xi)}{\left[2 - \xi^2 - \xi^3 + K_T^\infty - 3\xi^6 - \xi^8\right]} \quad (3)$$

with

$$\xi = \frac{D}{D + 2a_i} \quad (4)$$

with $i=s$ for the sandwich skin

$i=c$ for the skin coupon

and

$$K_T^\infty = 1 + \sqrt{2 \sqrt{E_x / E_y} - \nu_{xy} + E_x / 2G_{xy}} \quad (5)$$

Equation 1. was originally used to predict the variation of tensile strength due to a through the thickness hole (or notch) in a multi-ply laminate. The parameter a_i was introduced to represent a distance, characterizing the damage zone in the highly stressed region adjacent to the hole. The distance is used as a free parameter to be determined by fitting experimental data assuming an average stress over the damage zone. This criterion has been extended to include compression loaded laminates by Nuismer and Labor [4]. Two damage size-parameters have been used for the present investigation a_s for the sandwich configurations and a_c for the coupon configuration.

B. Comparison of the effect of impact damage with that of an open (drilled) hole .

The residual strength data which was shown in Figures 13 and 15 is replotted in Figure 18 as a function of the ratio of damage (open hole) size (D) and specimen width (W). The data for both series of flexural test beams show a similar dependence on D/W. The experimental results were therefore represented by a single curve, using the analytical open hole model of Equation 1, with $a_s = 9.3$ mm. as the curve fitting parameter.

This result indicates that the use of an open hole model for the prediction of post-impact compression strength is justified for the present case. It also means that the damage size (D) is the only parameter required and that the impact history (impact velocity, energy, load, etc.) does not need to be known to make quantitative residual strength predictions. This latter point is also substantiated by earlier findings [33,35].

C. Comparison of the effect of open holes in sandwich skins and skin coupons laminates.

The stress at failure of unnotched samples was used to normalize the strength data obtained on the two different specimen geometries used in test series #2 and #3. Figure 19 compares this normalized stress at failure as a function of the normalized hole size (D/W), which was also used to represent the data in Figure 18. Similar trends of strength loss with increasing D/W can be observed. The general trend appears to be that the sandwich skins lose their strength more gradually than the skin laminate coupons.

The respective analytical plots based on Equation 1 reveal two different empirical parameters; a higher one for the sandwich skin ($a_s=9.3\text{mm}$) and a lower one for the skin coupons ($a_c=2.7\text{mm}$). The parameter a_i may have a physical significance by quantifying the stress distribution shape and its singularity level and may be a measure of notch sensitivity. Hence, based on comparing the a values in the two cases it may be concluded that sandwich skins are much less sensitive to open-hole and impact damage as compared with skin laminates.

D. Net Strength Comparisons

The Net Strength (NS) is defined as the load carrying capacity of the material that remains in the cross section of the skin material after part of it has been taken out by impact or drilling. Its advantage is that local stress concentration effects can now be compared as a direct function of the damage size or hole diameter (D). This was done in Figure 20 for the "Normalized Net Strength" (NNS). Changes in NNS for sandwich skins were only minor for values of D above 4 mm (.16"). A continuous decrease in NNS is noticeable for skin coupons with values of D up to 10 mm (.39").

Additionally a Normalized Net Strength Loss (NLS) variable may be derived from NNS ($NLS=1-NNS$). It is plotted as function of hole diameter for both cases (Figure 21).

The sandwich skins, with $NSL_{max}=26\%$, clearly have a substantially better performance than the skin coupons with $NSL_{max}=42\%$.

The better residual compressive strength of damaged (open-hole) sandwich skins (in-situ) as compared with the respective performance of skin coupons is attributable to two possible reasons:

- 1) The presence of a supportive structural core stabilizes the skin resistance against a compressive sub-laminate buckling mechanism [43].
- 2) The presence of the core induces in-plane bi-axial compressive stress state in the skin which may improve its axial strength. [44,45].

CONCLUSIONS

An experimental investigation was conducted on three test configurations; two series of sandwich beams (post-impact and open-hole) loaded in flexure and a series of uniaxially loaded open-hole laminated coupons with the same composition as the sandwich skins.

The test results and analytical consideration lead to the following conclusions:

- The assumption that the localized impact damage, which is typical for sandwich construction with syntactic foam core, can be modeled as an open hole is justified. Engineers can therefore calculate the post impact strength of sandwich skins based on a simple open hole analysis model, in which the observed (measured) damage size is used as input.
- The residual compressive strength of post-impact and open-hole sandwich skins show a similar dependency on damage (hole) size. This can be attributed to the local nature of the

impact damage within the skin, as is typically observed in sandwich beams with syntactic foam core.

- The baseline data for sandwich skin coupons indicates lower strength as compared to sandwich data for the same hole size. Normalized Compressive Strength for open-hole sandwich skins and for laminate skin coupons follows a similar trend with increasing hole diameter.

- The Net Strength Loss (NSL) (derived from net stress at failure) is significantly higher for open-hole skin laminate coupons than for its sandwich skin counterparts.

-The higher performance of open hole (or impact damaged) sandwich skins is attributable to the better resistance of the skin to compressive sub-laminate buckling and to the biaxial state of stress in the skin, both effects which are due to the presence of the syntactic structural foam core.

ACKNOWLEDGMENT

The author would like to thank Dr. Howard Nelson, Roy Hampton, and Dave Chappell of the test Engineering and Analysis Branch at NASA Ames Research Center for their support and encouragement and to Paul Scharmen of the Model Development Branch at the Center for the high-level manufacturing of the specimens. Additionally, the contributions of Mike Luft in keeping track of the experimental data and making plots are greatly appreciated.

References

- [1] Lekhnitskii, S. G., " Anisotropic Plates " translated from the second russian edition by Tsai, S.W., and Cheron, T., Gordon and Breach Science Publishers, New York. 1968, pp. 171-190. Original publication in russian, 1957.
- [2] Savin, G.N., " Stress distribution around holes" Translated from russian, NASA TT F-607 , 1970, pp. 227-324 . Original publication in russian, 1968.
- [3] Whitney, J.M., and Nuismer, R.J., "Stress fracture criteria for laminated composites containing stress concentrations". *J. of Composite Materials* Vol. 8 July 1974, pp. 253-265.
- [4] Nuismer, R.J. and Labor, J. D. , " Application of the average stress failure criterion: Part II - Compression," *J. of Composite Materials*, Vol. 13, Jan. 1979, pp. 49-60.
- [5] Sun, C.T. and Lao, J., " Failureloads for notched graphite/epoxy laminates with a softening strip, " *Composite Science and Technology*," Vol. 27, 1985, pp. 121-133.
- [6] Lubowinski, E. G., Guynn, W. E., and Whitcomb, J. D., " Loading rate Sensitivity of open hole composites in compression," NASA TM 100634, August 1988, 30p.
- [7] Guynn, E. G. and Bradley, W. L., "A detailed Investigation of the micromechanisms of compressive failure in open hole composite laminates," *J. of Composite Materials*," Vol. 23, May 1989, pp. 479-504.
- [8] Guynn, E. G. and Bradley, W. L., Measurements of the stress supported by the crush zone in open hole composite laminates loaded in compression," *J. of Reinforced Plastics and Composites*, Vol. 8, March 1989, pp. 133-149.
- [9] Larson, Per-Lennart, " On buckling of orthotropic stretched plates with circular holes," *Composite Structure*, Vol.11, 1989, pp. 121-134.
- [10] Lin, C.C. and Kao, C.S., "Buckling of laminated plates with holes," *J. of Composite Materials*, Vol. 23, June 1989, pp. 536-553.

- [11] Chang, F. K. and Lessard, L. B., "Damage tolerance of laminated composites containing an open hole and subjected to compressive loadings: Part I--Analysis," *J. of Composite Materials*, Vol. 25, Jan. 1991, pp. 2-43.
- [12] Lessard, L. B. and Chang, F. K., "Damage tolerance of laminated composites containing an, open hole and subjected to compressive loadings: Part II: Experimental," *J. of Composite Materials*, Vol. 25, Jan. 1991, pp. 44-64.
- [13] Chang, F. K., Scott, R.A. and Springer, G. S., "Strength of Mechanically Fastened Composite Joints," *J. of Composite Materials*, Vol. 16, Nov. 1982, pp.470-494.
- [14] Chang, F. K. and Scott, R.A., " Failure of composite laminates comntaining pin loaded hole-method of solution," *J. of Composite Materials*, Vol. 18, May 1984, pp. 255-289.
- [15] Mahajerin, E. and Sikarskie, D. L., "Boundary element study of a loaded hole in an orthotropic plate," *J. of Composite Materials*, Vol. 20, July 1986, pp. 375-389.
- [16] Tsujimoto, Y. and Wilson, D., "Elasto-plastic failure analysis of composite bolted joints," *J. of Composite Materials*, Vol. 20, May 1986, pp. 236-252.
- [17] Erikson, I., " On bearing strength of bolted graphite/epoxy laminates," *J. of Composite Materials*, Vol. 24, Dec. 1990, pp. 1246-1269.
- [18] Tsai, S. W., "Composite Design" Fourth Edition, Think Composites: Dayton, Paris, and Tokyo. 1988, Section 18.
- [19] Williams, J. G. "Tough Composite Materials; Effect of impact damage and open holes on the compression strength of tough resin/high strain fiber laminates." NASA Conference Publication 2334, 1984, pp 61-79
- [20] Chamis, C. C. and Ginty, C. A., " Fiber composite structural durability and damage tolerance: Simplified predictive methods", *ASTM STP 1012*, 1989, pp. 338-355.

- [21] Jegley, D. C., "Compression behavior of graphite-epoxy and graphite-thermoplastic panels with circular holes or impact damage" NASA Conference Publication 3087 Part 2, 1990, pp. 537-558.
- [22] Hsi-Yung T.W. and Springer, G. S., " Measurements of matrix cracking and delamination caused by impact on composite plates" *J. of Composite Materials*, Vol. 22, June 1988, pp. 518-532.
- [23] Hsi-Yung T.W. and Springer, G. S., " Impact induced stresses, strains, and delaminations in composite plates" *J. of Composite Materials*, Vol. 22, June 1988, pp. 533-560.
- [24] Lesser, A. J. and Filippov, A. G., " Kinetics of damage mechanism in laminated composites" 36th International SAMPE Symposium, April 1991, pp. 886-899.
- [25] Starnes, J.H. and Williams, J. G., Failure characteristics of graphite-epoxy structural components loaded in compression" NASA Technical Memorandum 84552. 1982, 24 p.
- [26] Chai, H. and Babcock C. D., "Two-dimensional modelling of compressive failure in delaminated laminates", *J. of Composite Materials*, Vol. 19, Jan. 1985, pp. 67-98.
- [27] Marshall, R. D., Sandorff, P. E. and Lauraitis, K. N., "Buckling of a damaged sublaminates in an impacted laminate" *ASTM J. of Composite Technology & Research* Vol. 10, No. 3, Fall 1988, pp. 107-113.
- [28] Ishai, O. and Shragai, A. " Effect of impact loading on damage and residual compressive strength of CFRP laminated beams", *Composite structures*, Vol. 14, 1990, pp. 319-337
- [29] Shalev, D. and Reifsnider, K.L., "Study of the onset of delamination at holes in composite laminates", *J. of Composite Materials*, Vol. 24 Jan. 1990, pp. 42-71.
- [30] Soutis, C. and Fleck, A.F., " Static compression failure of carbon fiber T800/924C composite plate with single hole", *J. of Composite Materials*, Vol. 24 , may 1990, pp. 536-558.

- [31] Gottesman, T., Bass, M. and Samuel, A., "Critically of Impact Damage in Composite Sandwich Structure," 6th International Conference of Composite Materials, Vol. 3, 1988, pp. 327-335 .
- [32] Sommers, M., Weller, T., and Abramovich, H., "Influence of predetermined dalaminations on buckling behavior of composite sandwich beams," *Composite Structures*, Vol. 17. 1991, pp. 292-329.
- [33] Kim, C. G., AND Jun, E. J., " Impact resistance of composite laminated sandwich plates", *J. of Composite Materials*, Vol. 26, No. 15, 1990, pp. 2247-2261.
- [34] Abrate, S. "Impact on laminated composite materials", *Appl. Mech. Rev.* Vol. 44, No. 4 April 1991.
- [35] Ishai, O., and Hiel, C. "Damage tolerance of a composite sandwich with interleaved foam core," *ASTM J. of Composite Technology & Research JCTRER*, Vol. 14, No. 3, Fall 1992, pp. 155-168.
- [36] Hiel, C. and Ishai, O., "Design of highly damage-tolerant sandwich panels," 37th International SAMPE Symposium, March 1992, pp. 1228-1242.
- [37] SACMA Recommended Test Method for Open-Hole Compression Properties of Oriented Fiber-Resin Composites. Recommended method, SRM 3-88.
- [38] Standard Tests for Toughened Resin Composites Revised Edition, NASA Reference Publication 1092, July 1983, 35 pages.
- [39] SACMA Recommended Test Method for Compressive Properties of Oriented Fiber-Resin Composites. Recommended Method, SRM 1-88.
- [40] Whitney, J.M. and Guihard S. K. " Failure modes in compression testing of composite materials," 36th International SAMPE Symposium, April 1991, pp. 1069-1078.
- [41] Daniel, I. M., " Behavior of graphite/epoxy plates with holes under biaxial loading," *Experimental Mechanics*, Vol. 20, No. 1, Jan. 1980, 8 pages.
- [42] Daniel, I. M., " Biaxial testing of $[0_2/\pm 45]_s$ graphite/epoxy plate with hole," *Experimental Mechanics*, Vol. 22, No. 5, may. 1982, 8 pages.
- [43] Gillespie, J.W., and Carlson, L.A., "Influence of finite width on notched laminate strength predictions," *Composites Science and Technology*, Vol 32, 1988.

List of Captions

- Fig. 1 Detailed description of non-damaged (Virgin) sandwich beam configuration.
- Fig. 2: Illustration of specimen configurations for the different test series
- Fig. 3: Flexural test set-up.
- Fig. 4 : Low velocity Impact test set-up:
- Fig. 5: Compression Loading device for standard testing of virgin skin specimens.
- Fig. 6: Compression Loading device for standard testing of open-hole skin specimens.
- Fig. 7: Stress Distribution and formulation for hybrid skin laminate under uniaxial compression.
- Fig. 8 : Stress Distribution and formulation for hybrid sandwich beam under flexure.
- Fig. 9: External damage imprint on sandwich skin due to low velocity impact loading.
- Fig. 10 :SEM of Typical Cross-section with low velocity impact damage (Impact energy: 90J)
- Fig. 11: Micro graphs of cross-section of sandwich specimens damaged under different levels of impact energies
- Fig. 12: The effect of low velocity impact energy on visible damage size of sandwich beams with syntactic foam core.
- Fig. 13: The effect of damage size on Nominal residual strength of post-impact sandwich (series 1).
- Fig. 14: Typical failure modes for: a) Impact-damaged sandwich beam under flexure
b) Open-hole skin of sandwich beam under flexure
c) Open-hole skin coupon under uniaxial compression.
- Fig 15: Effect of hole diameter on nominal strength of open-hole sandwich specimens (series 2).
- Fig. 16: Effect of hole diameter on nominal strength of open-hole skin coupons (series 3)
- Fig. 17: Open-hole model and formulation for prediction of compressive strength.
- Fig. 18: Comparison of impact damage and open hole effects on residual strength of sandwich beams.
- Fig. 19: Comparison of open-hole size per unit width effects on normalized nominal compressive strength for sandwich beams vs. skin coupons.

Fig. 20: Comparison of the effect of open-hole size on normalized net compressive strength for sandwich beams vs. skin coupons.

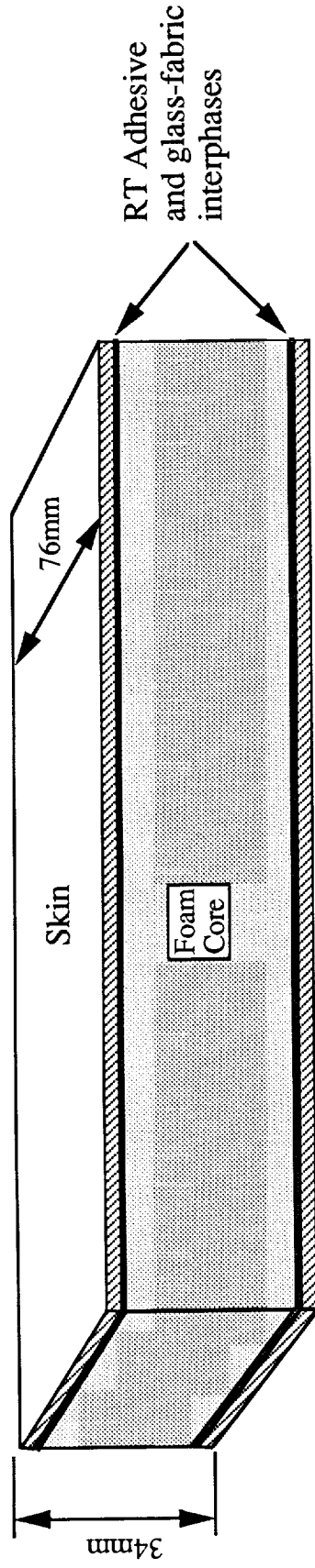
Fig. 21: Comparison of the effect of open-hole size on net compressive strength loss for sandwich beams vs. skin coupons.

MATERIAL	ELASTIC PROPERTIES			STRENGTH PROPERTIES						C.T.E		Thickness mm
	GPa			MPa						$^{\circ}\text{C}^{-1} \times 10^{-6}$		
	E11	E22	G12	v12	F1t	F1c	F2t	F2c	F6	$\alpha 1$	$\alpha 2$	t0
CFRP G40-600 5245C (U.D. Lamina)	170	12	5.2	0.33	2070	1380	75	251	102	-0.3	28	0.14
GFRP Fabric 7781 5245C	30	30	5.4	0.17	374	560	374	560	99	9.9	9.9	0.24
Syntactic Foam 350C	2.3	2.3	1.1	0.31	26	55	26	55	26	32	32	25
Adhesive FM300 (0.08psf)	2.5	2.5	0.89	0.38	61	74	61	74	35	77	77	0.26
CFRP Laminate (0/30/-30) _{3s} (**)	97	15	25	1.2	936	650	70	289	153	-2.7*	19*	2.5

*) Coefficient of Thermal Expansion values were determined experimentally at a temperature range of 20-120°C

**) Most CFRP Laminate properties were computed based on the respective lamina inputs except $\alpha 1$, $\alpha 2$, and F1c which were derived experimentally

Table 1 : SANDWICH CONSTITUENT PROPERTIES



Skins composition : CFRP - Rigidite 5245C/G40-600 Lay-up : (0 /+30/-30) ^{3s}
 + GFRP Fabric - 7781-5245C - 2 layers on each side of CFRP

Core composition : Syntactic foam - Syntac 350 (glass microballoons in epoxy resin)

Interphases composition : Hysol EA9394 Adhesive

Figure 1 : Sandwich Beam Configuration

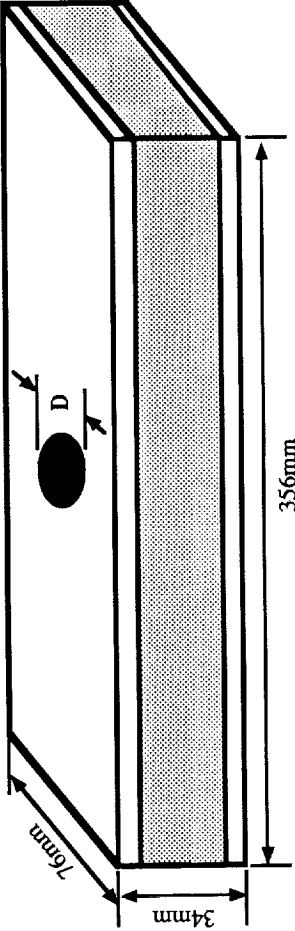
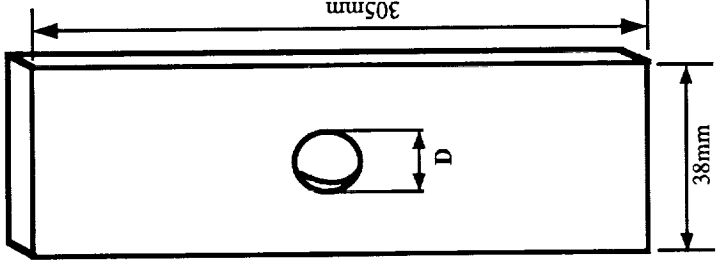
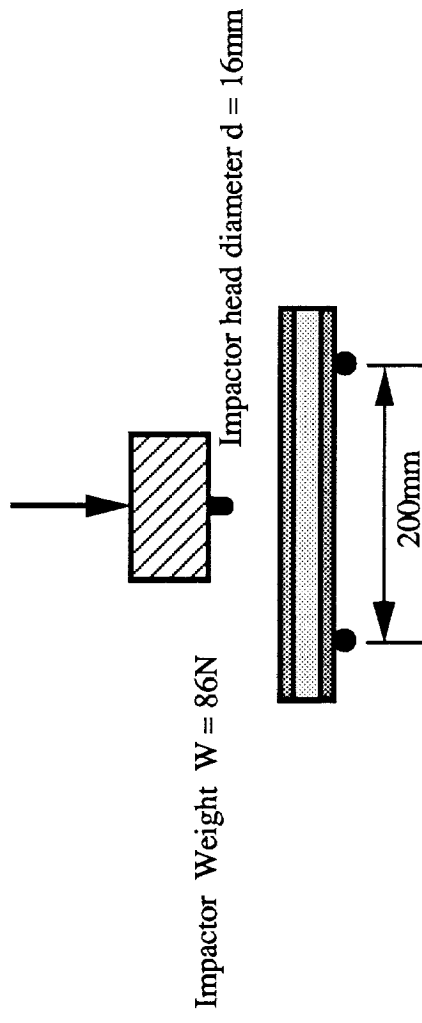
Sandwich Skin Laminate		Skin Coupon Laminate
Post Impact	Open Hole	Open Hole
		

Figure 2 : Specimen Configurations



Velocity range : Up to 6 m/s

Energy range : Up to 180 J

Figure 3 : Low Velocity Impact Test Set-Up

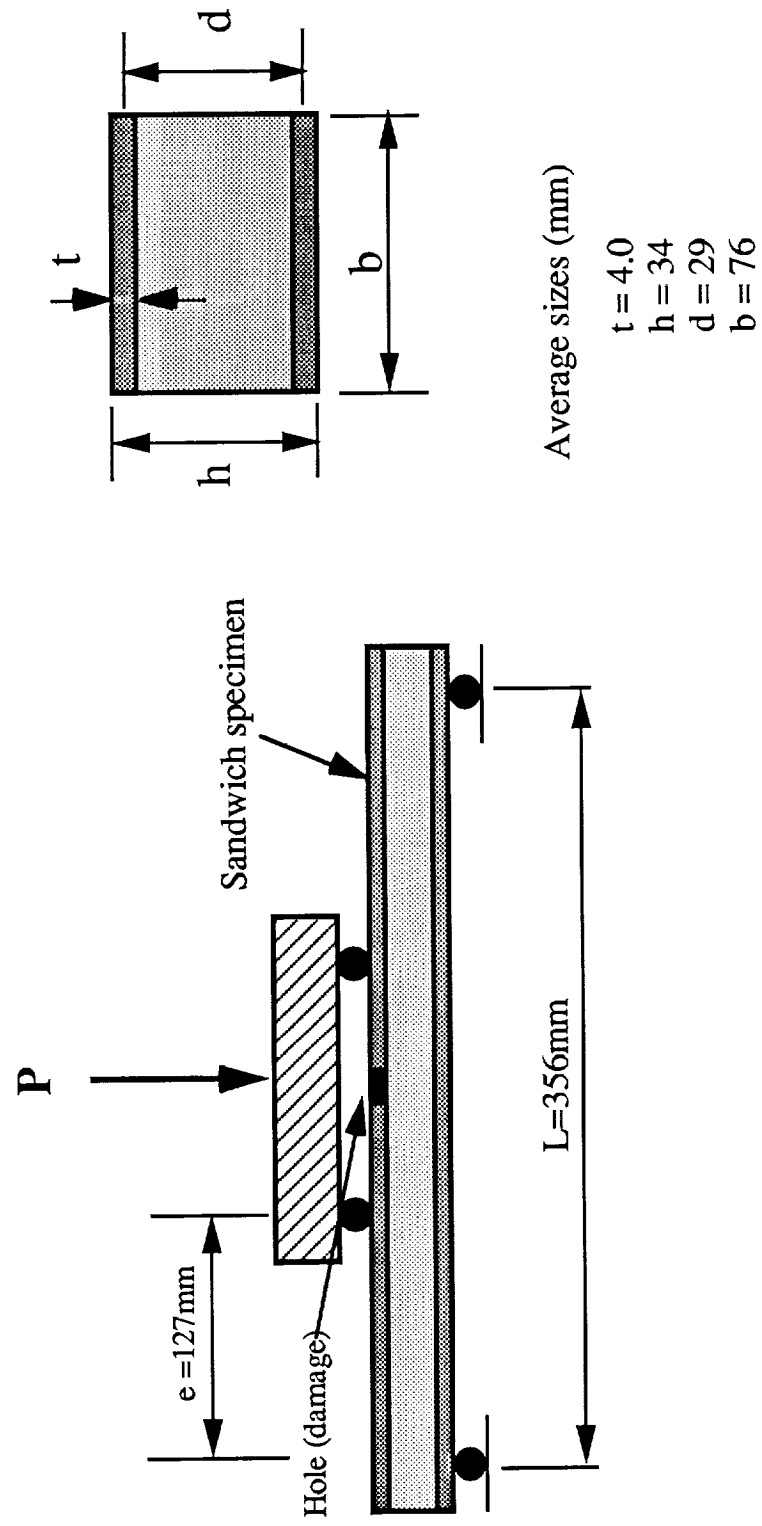


Figure 4 : Flexural Test Set-Up

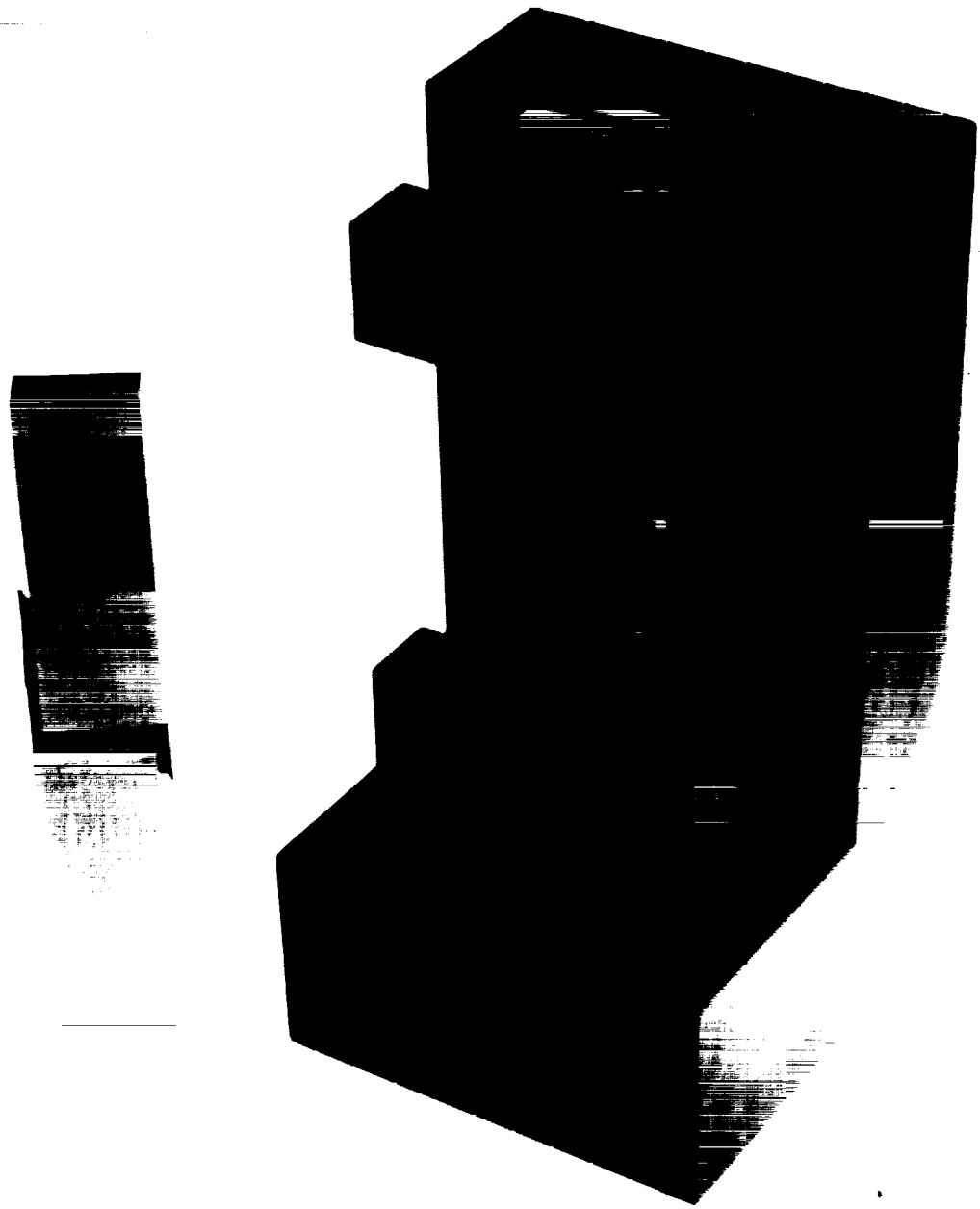


Figure 5. Compression Loading device for standard testing of virgin specimen



Figure 6. Compression loading device for standard testing of open-hole skin specimens

ORIGINAL PAGE

BLACK AND WHITE PHOTOGRAPH

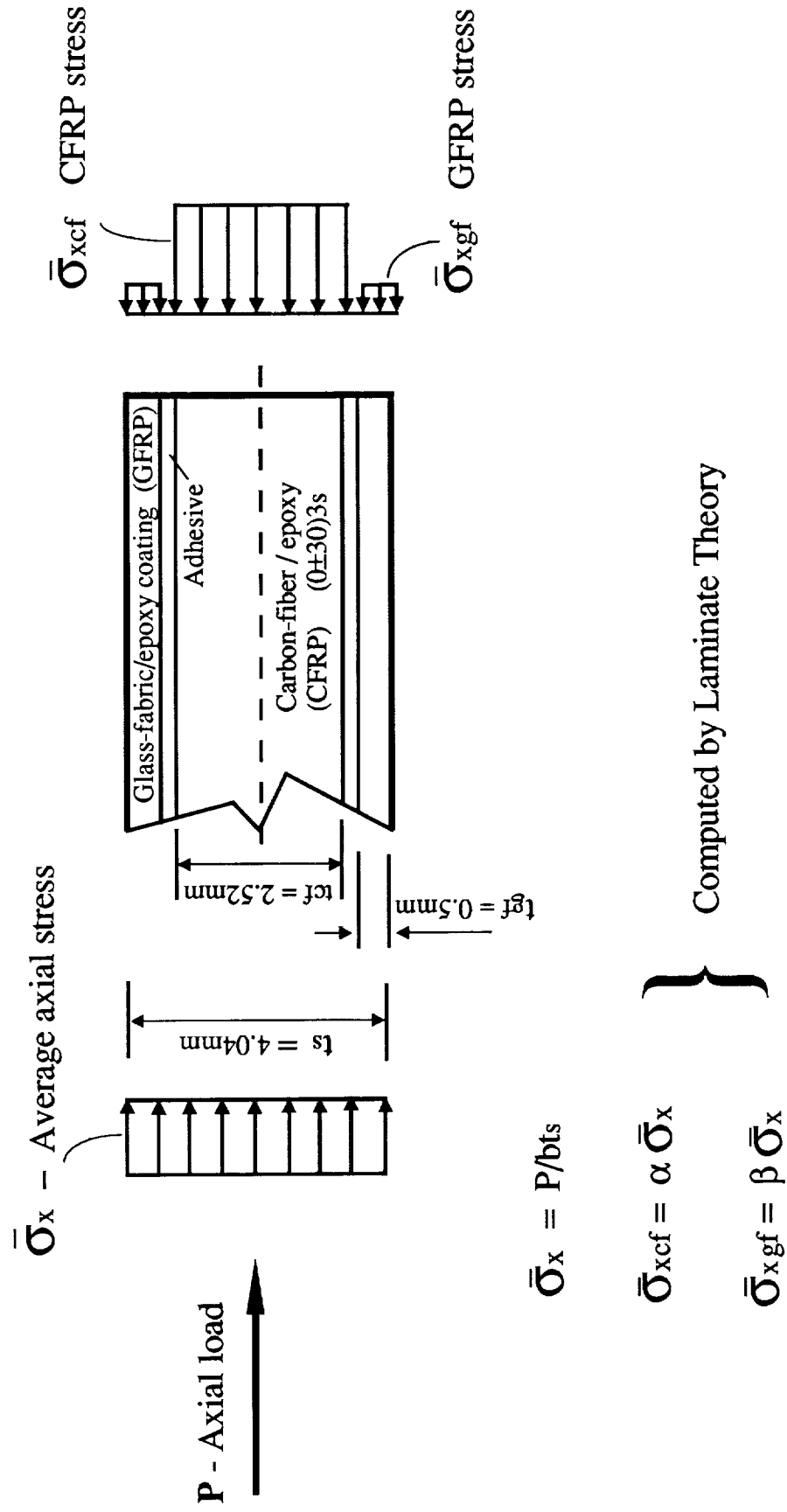


Figure 7: Stress Distribution in CFRP/GFRP Skin Specimen Under Uniaxial Loading

Approximate formulation

$$\bar{\sigma}_{cf} = M h_{cf} / b t_s d^2$$

$$d = h_{core} + t_s$$

Accurate solution
(Laminate theory)

$$\sigma_{cf} = \gamma \bar{\sigma}_{cf}$$

where $\gamma = 0.882$

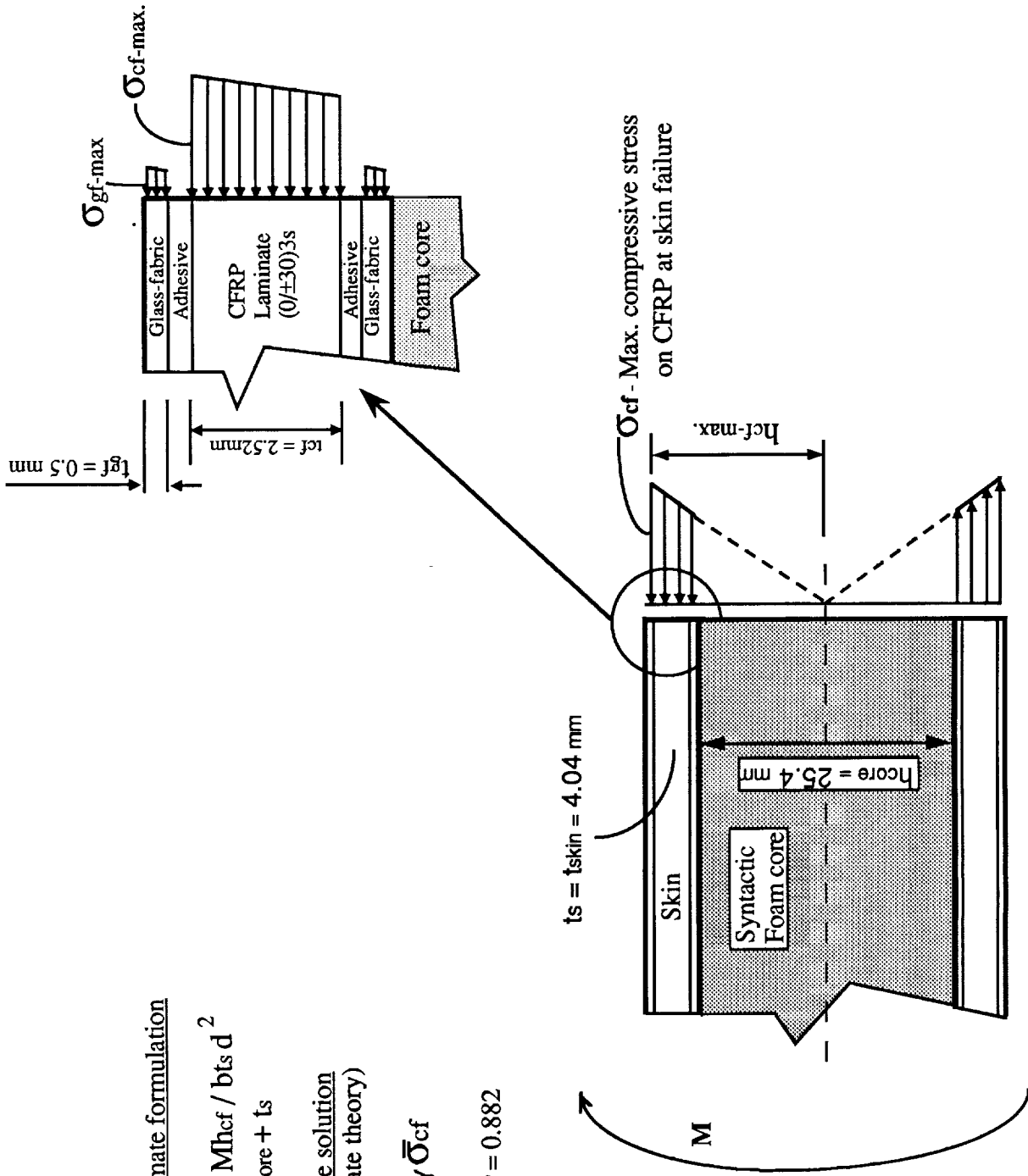


Figure 8 : Stress Distribution in CFRP/GFRP Skin in Sandwich Beam Under Flexure

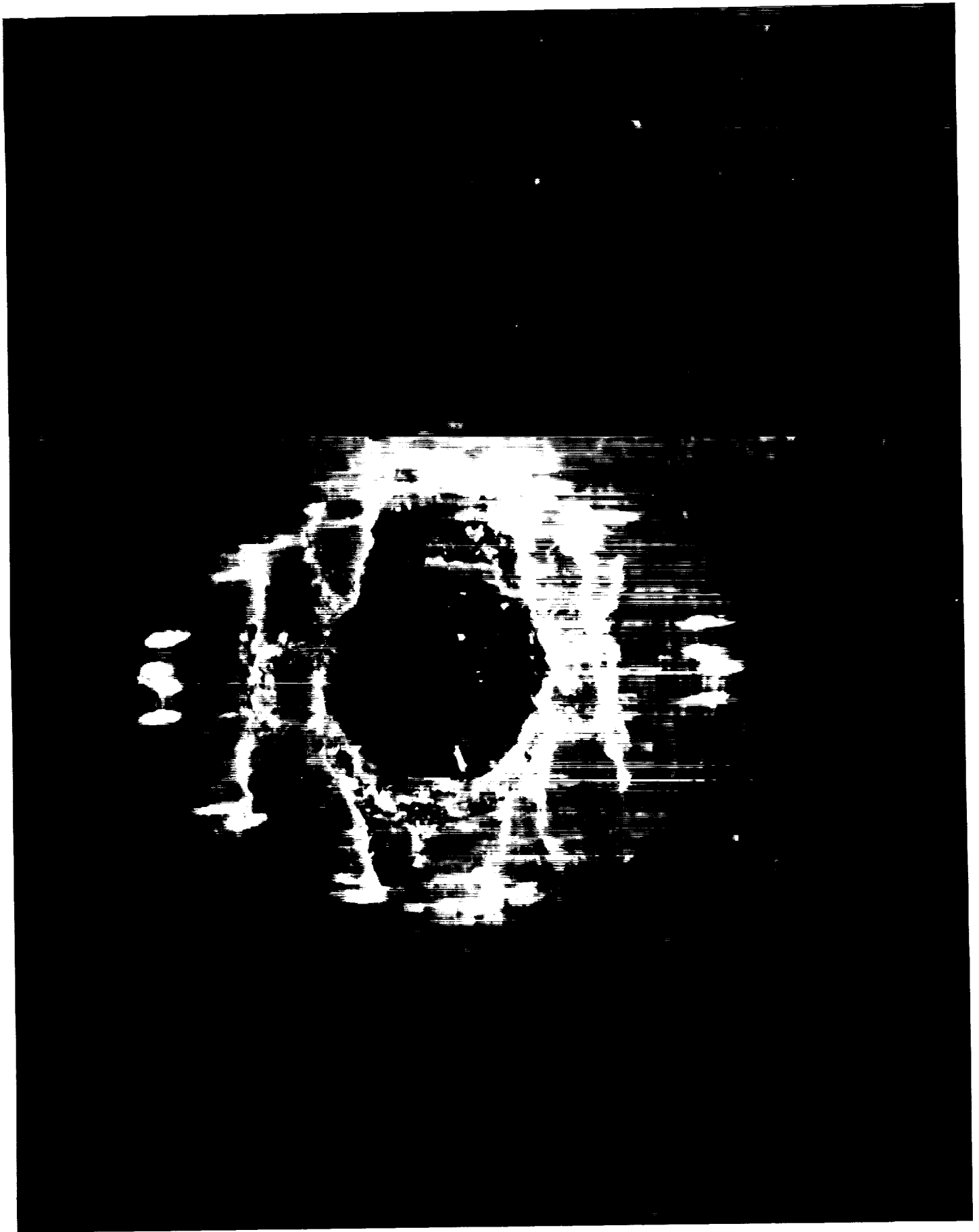


Figure 9. External damage imprint on sandwich skin due to low velocity impact loading

ORIGINAL PAGE
BLACK AND WHITE PHOTOGRAPH

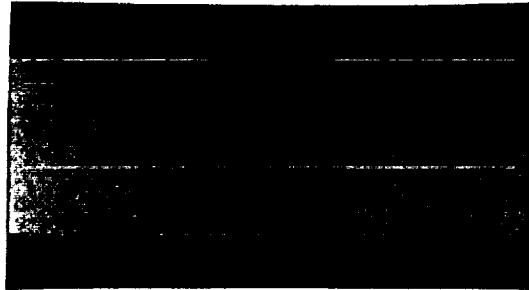


ORIGINAL PAGE
BLACK AND WHITE PHOTOGRAPH

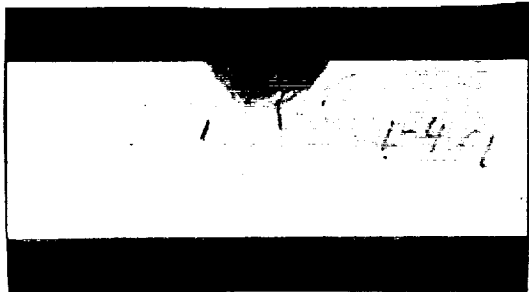
Figure 10. SEM of typical cross section with low velocity impact damage (impact energy=90 J)



47 J (34 ft-lb)



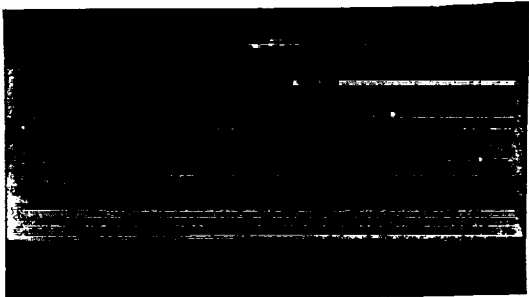
69 J (51 ft-lb)



90 J (67 ft-lb)



136 J (100 ft-lb)



180 J (132 ft-lb)

Figure 11. Micrographs of cross-section of sandwich specimens damaged under different levels of impact energy

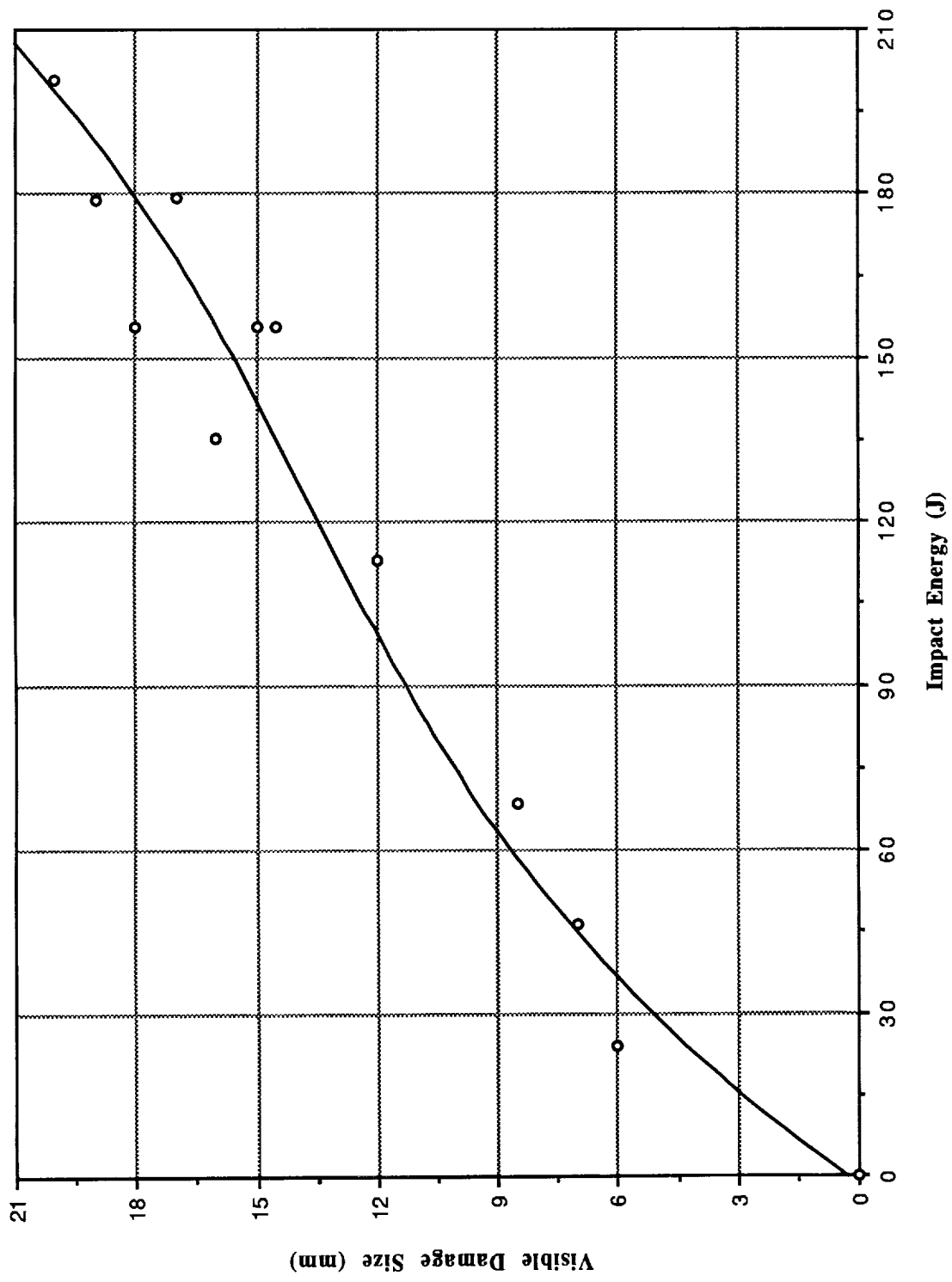


Figure 12 : Effect of Low Velocity Impact Energy on Visible Damage Size of Sandwich Skin

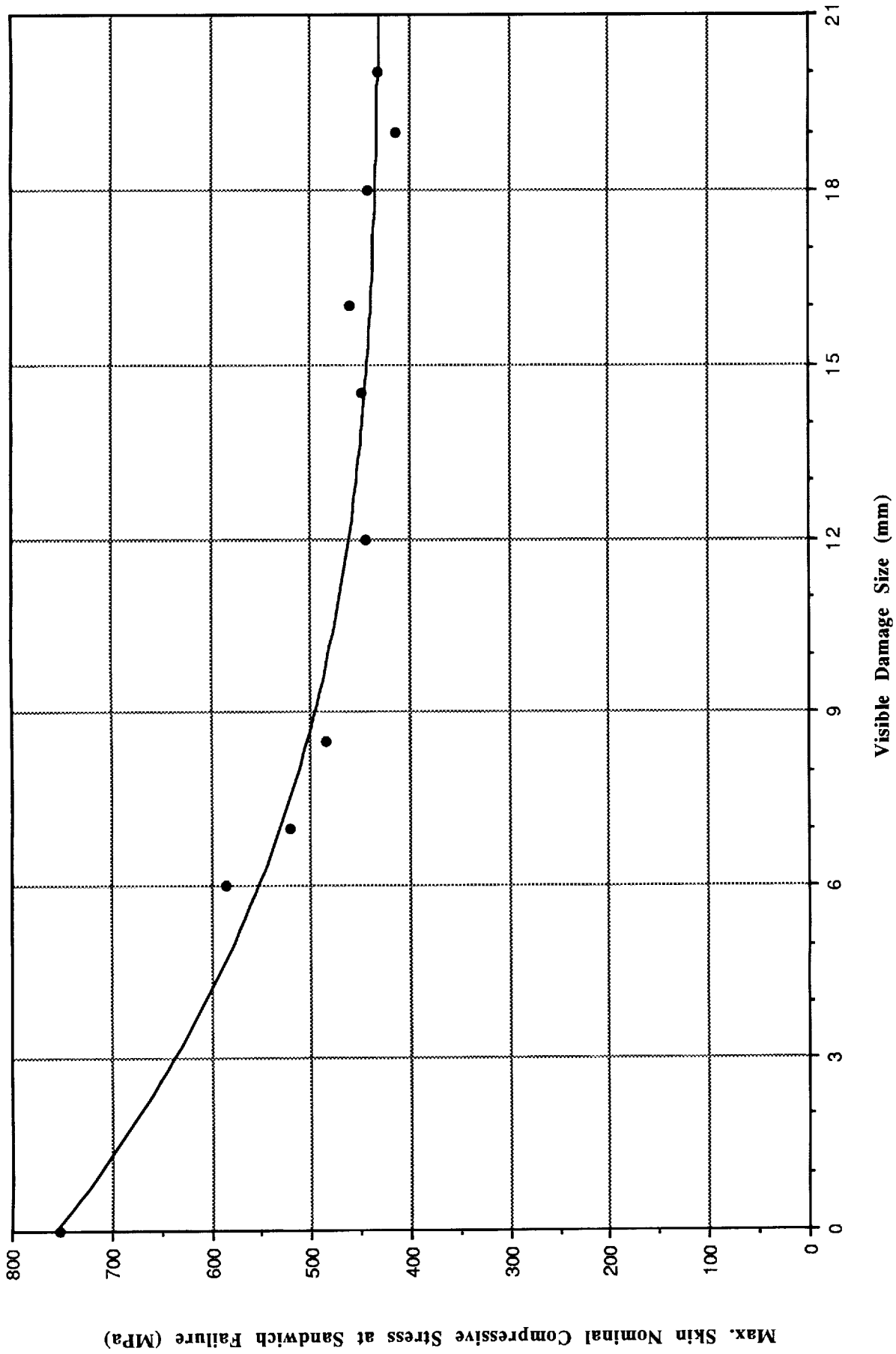


Figure 13 : Effect of Visible Damage Size on Nominal Compressive Strength of Sandwich Skin

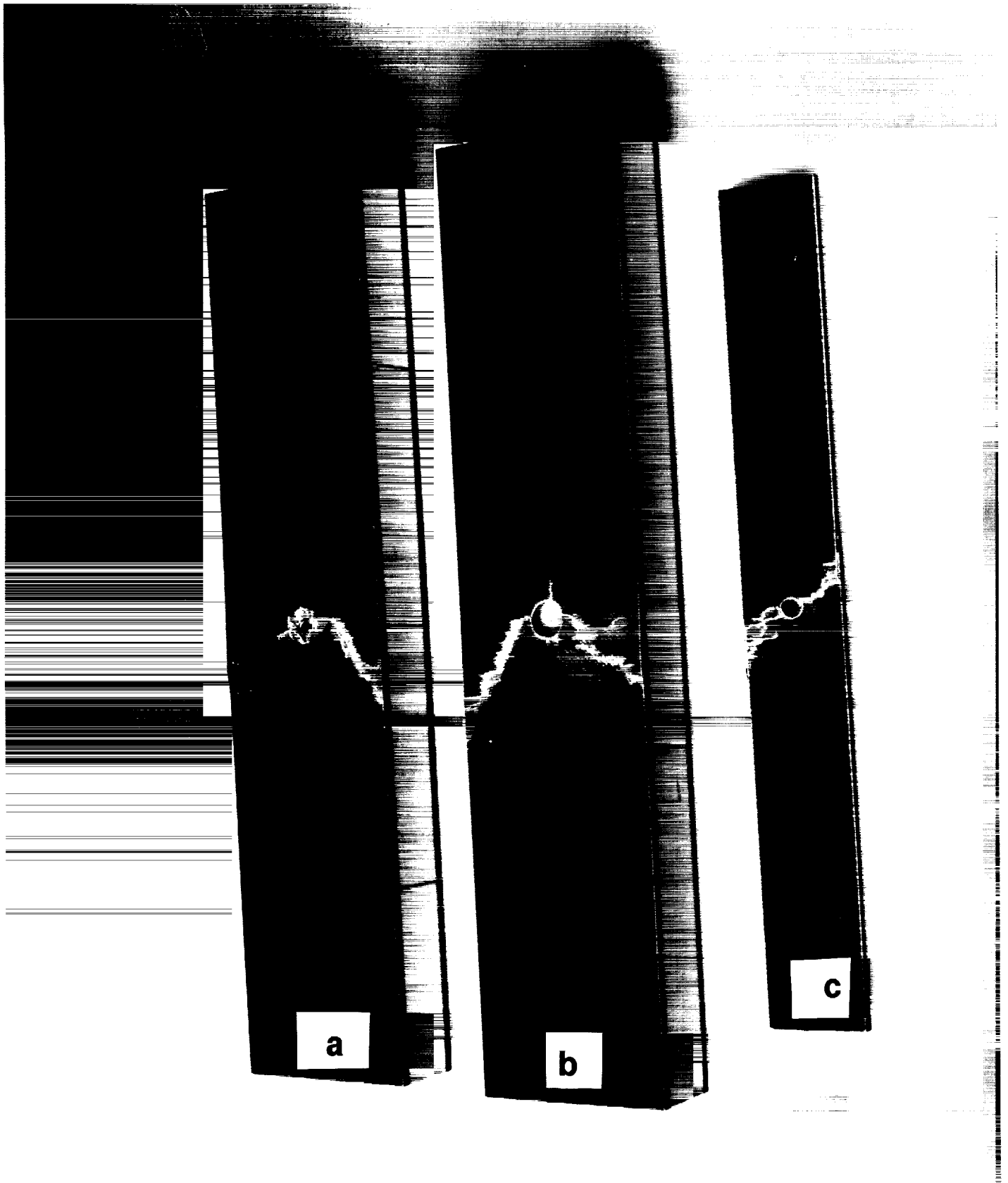


Figure 14. Typical failure modes for:a)Impact-damaged sandwich beam/b)open hole skin /c)open hole coupon

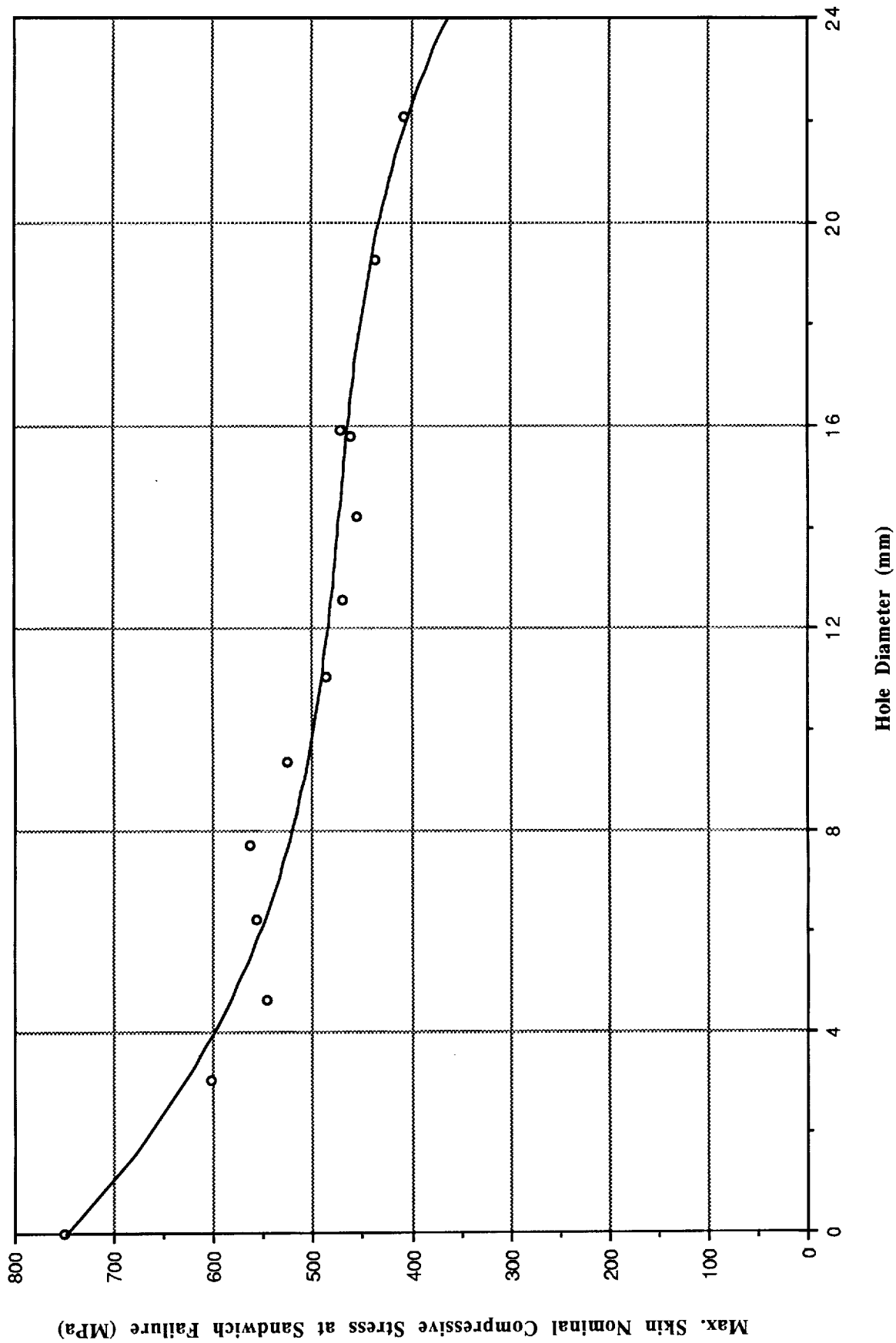


Figure 15 : Effect of Drilled Hole Diameter on Nominal Compressive Strength Sandwich Skins

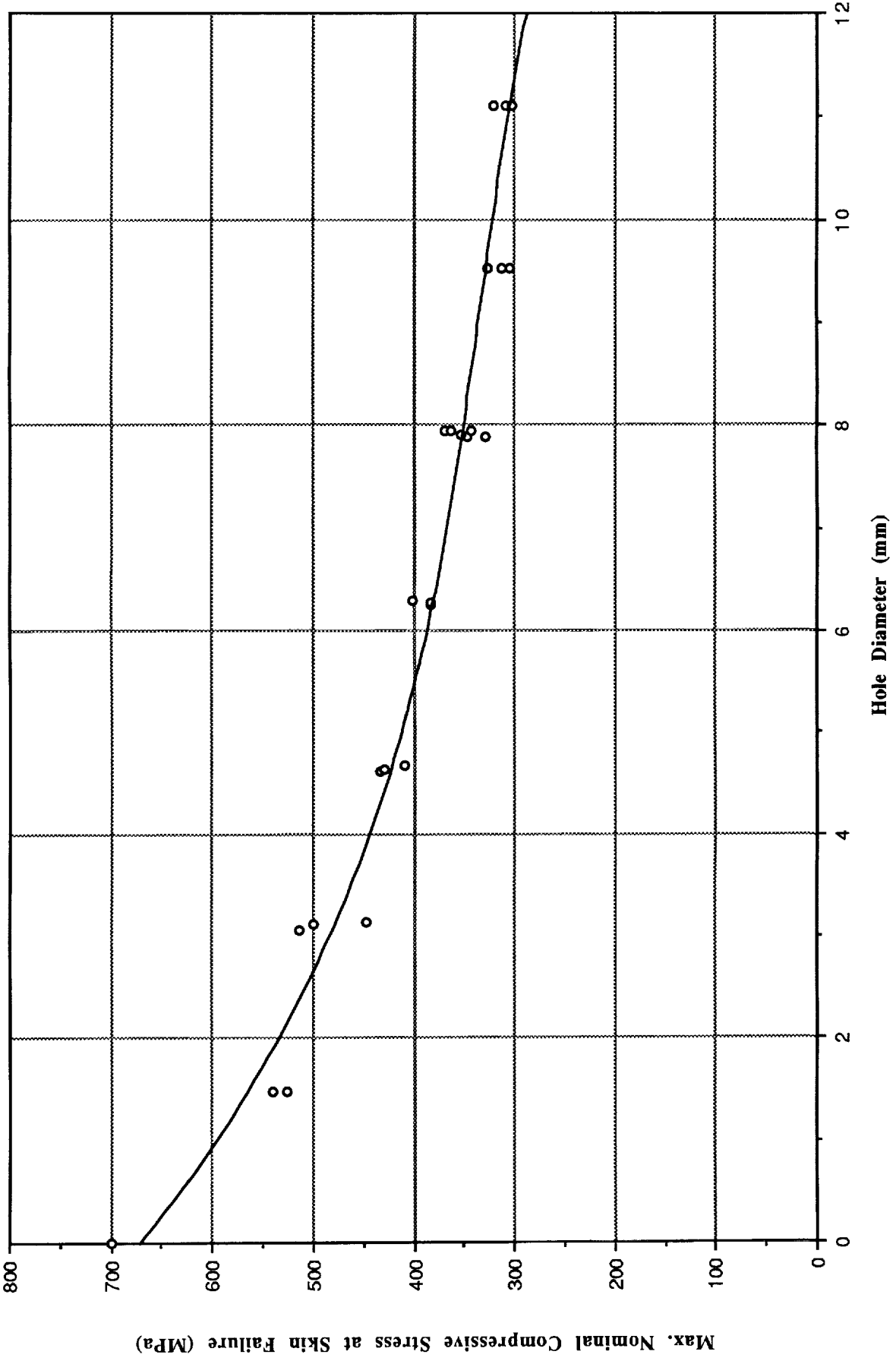


Figure 16 : Effect of Drilled Hole Diameter on Nominal Compressive Strength of Skin Coupons

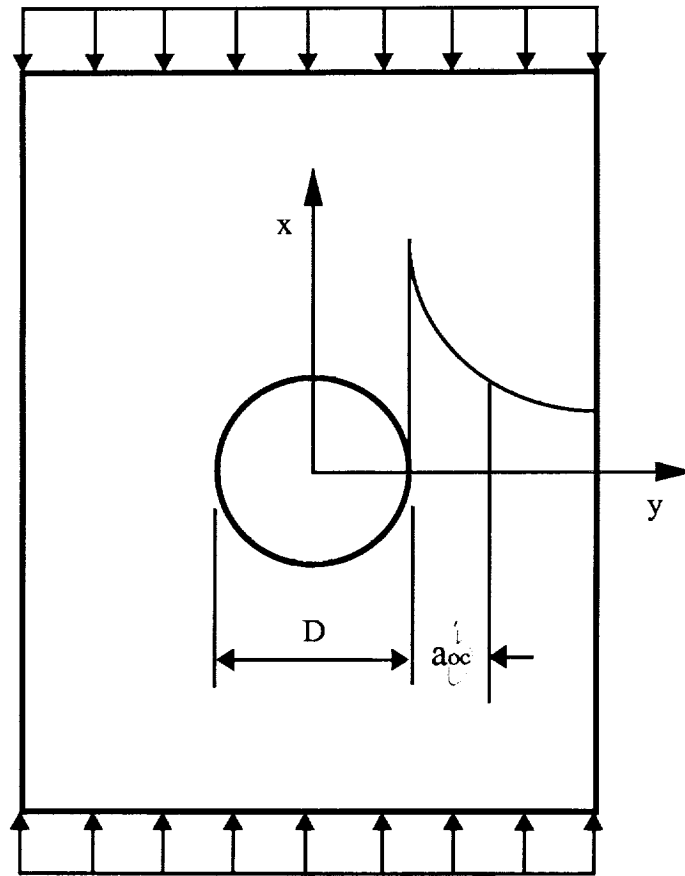


Figure 17 : Open Hole Model and Formulation for Prediction of Compressive Strength.

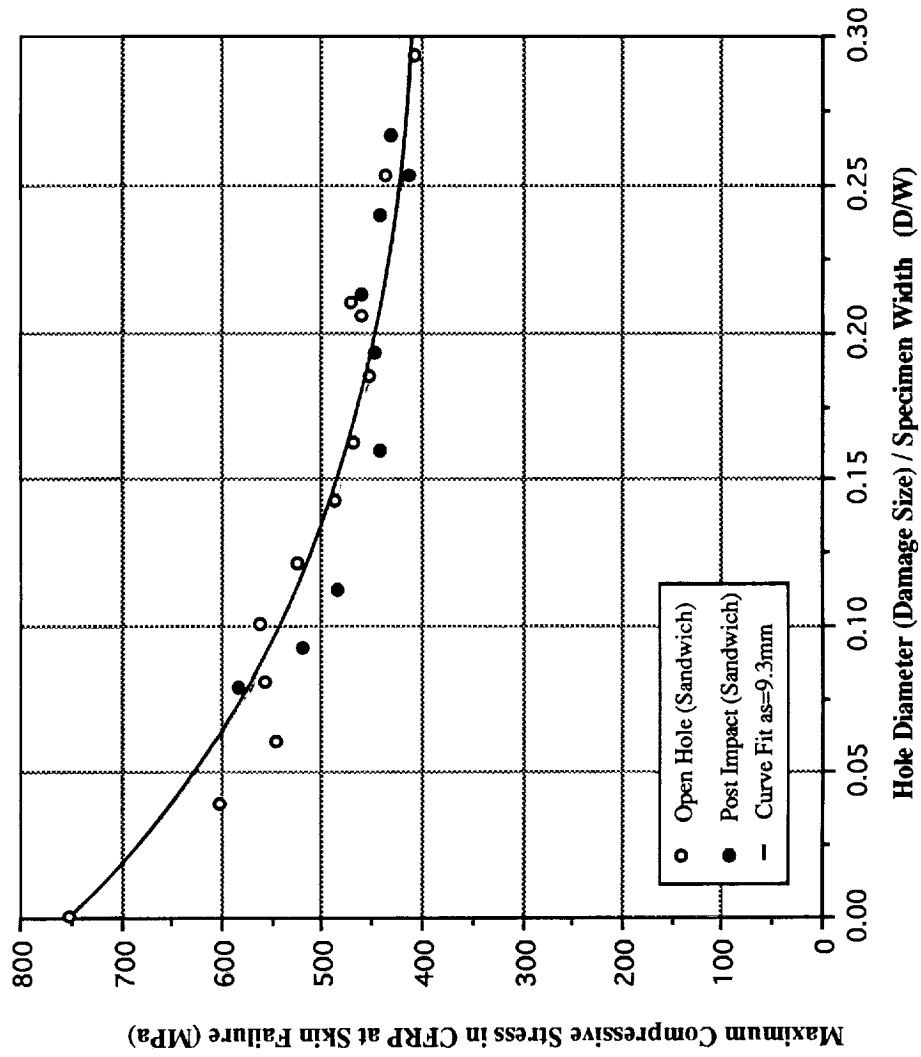


Figure 18: Post Impact and Open Hole Compressive Strength of Sandwich Beams in Flexure

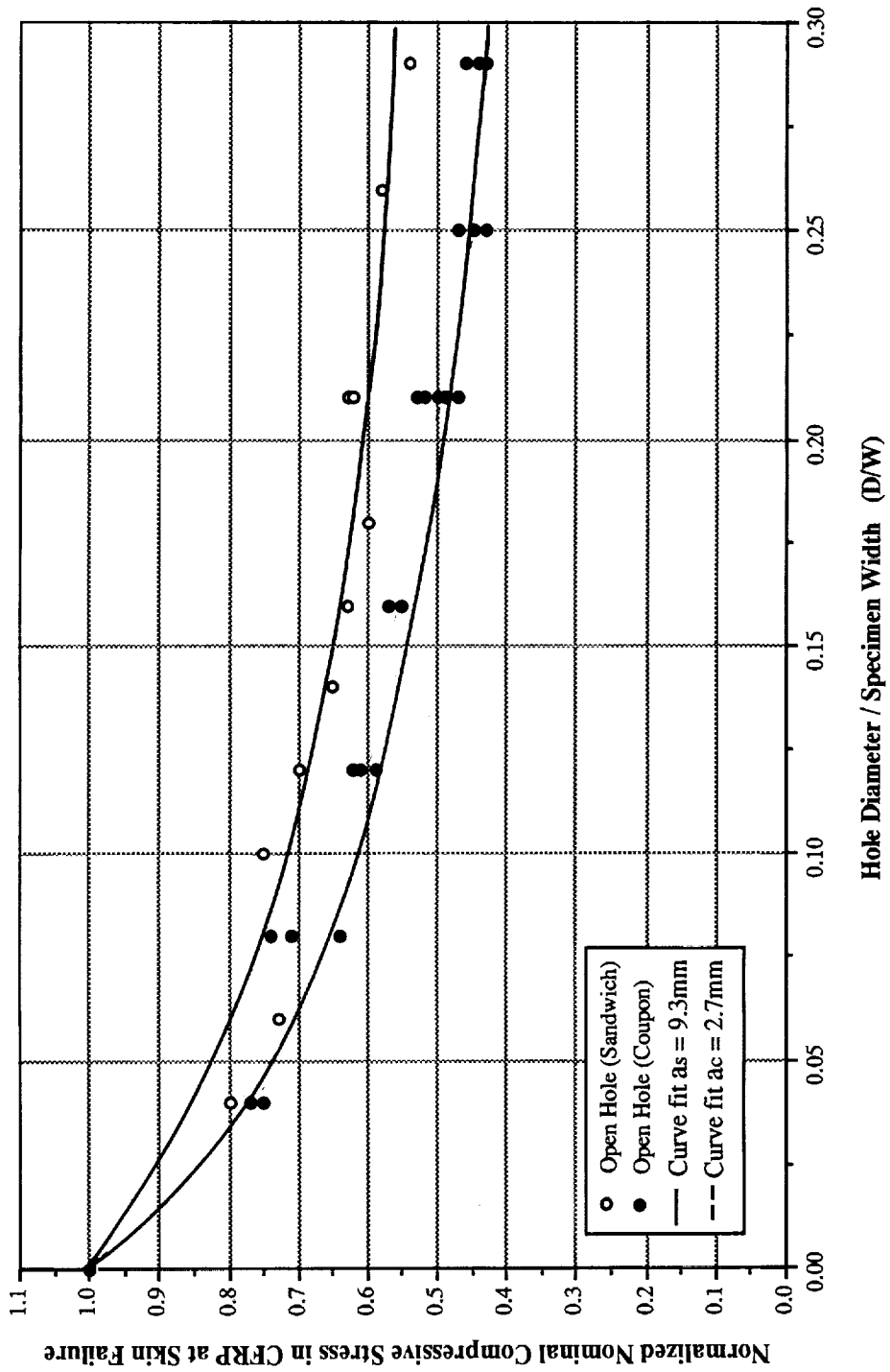


Figure 19: Comparison of Open Hole Nominal Compressive Strength (Normalized) for a Sandwich Skin Laminate vs. Skin Coupon Laminate

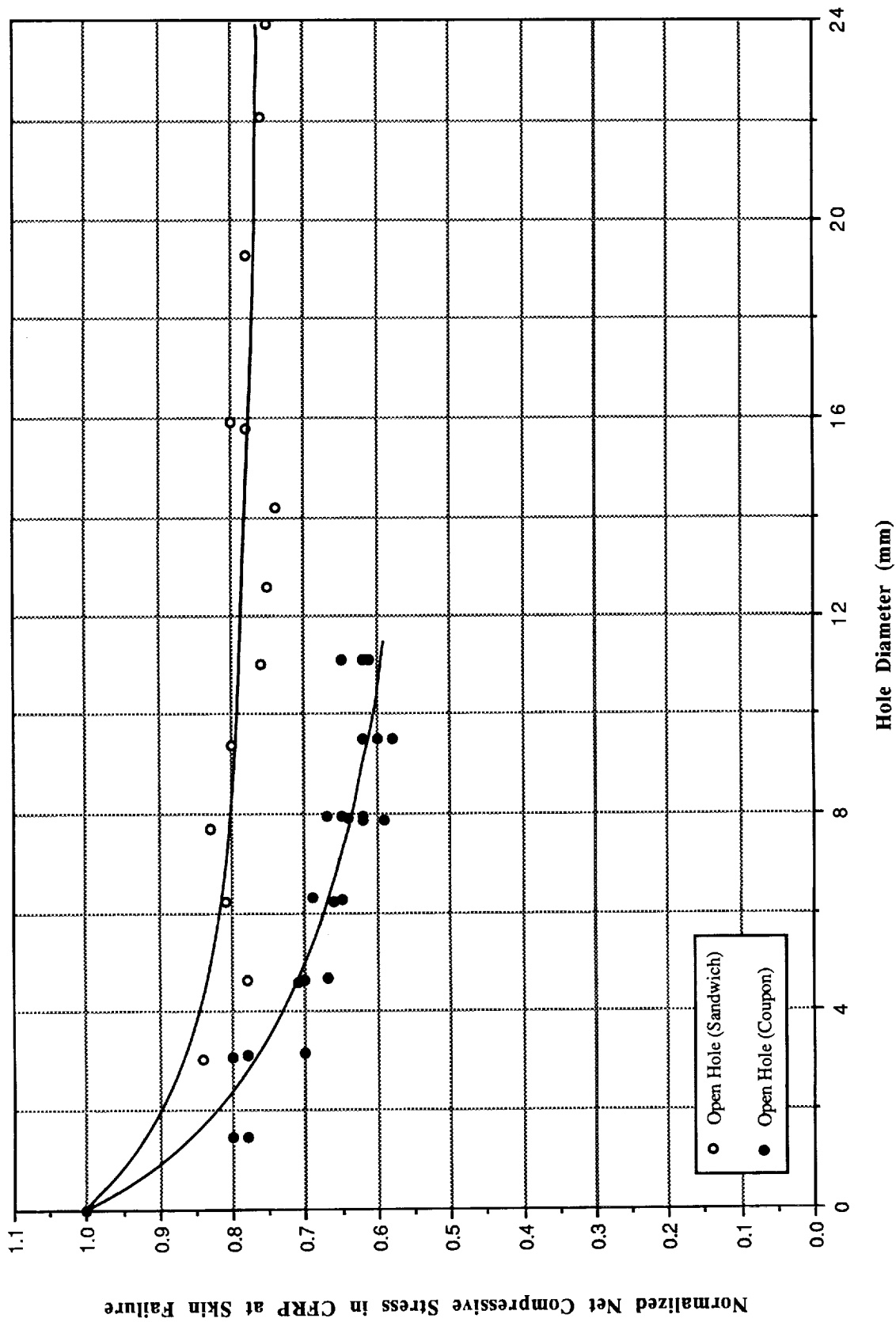


Figure 20: Comparison of Open Hole Net Compressive Strength (Normalized) for Sandwich Skin Laminate vs. Skin Laminate

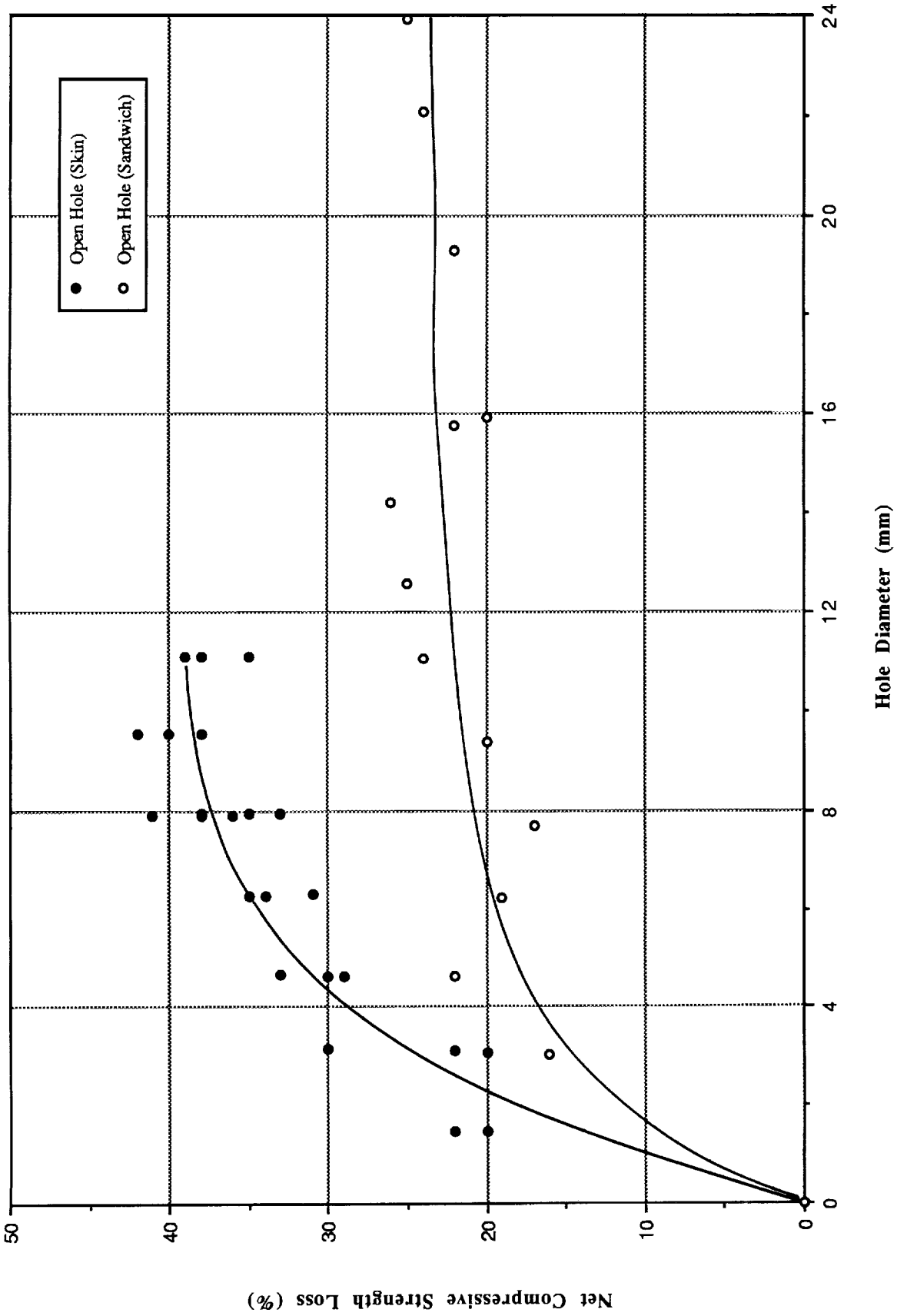
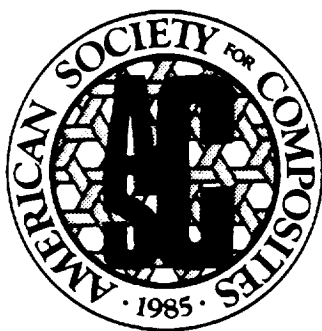


Figure 21: Net Strength Loss vs. Hole Diameter

II Appendix

**Papers published during grant period
June 1, 1992 - May 31, 1993**

PROCEEDINGS OF THE AMERICAN SOCIETY FOR COMPOSITES



SEVENTH TECHNICAL CONFERENCE

COMPOSITE MATERIALS, MECHANICS AND PROCESSING

Co-Sponsored by
PENNSYLVANIA STATE UNIVERSITY
THE COMPOSITES MANUFACTURING TECHNOLOGY CENTER
and
BOEING HELICOPTERS

October 13-15, 1992
Keller Conference Center
University Park, Pennsylvania



TECHNOMIC
PUBLISHING CO., INC.
LANCASTER • BASEL

The logo for Technomic Publishing Co., Inc. features a stylized 'T' and 'M' symbol above the company name. Below the company name, the locations 'LANCASTER • BASEL' are listed.

Low and High Velocity Impact Response of Thick Hybrid Composites

C. HIEL AND O. ISHAI
NASA Ames Research Center
MS 213-3
Moffett Field, CA 94035

ABSTRACT

The effects of low and high velocity impact on thick hybrid composites (THC's) were experimentally compared. Test Beams consisted of CFRP skins which were bonded onto an interleaved syntactic foam core and cured at 177°C (350 °F). The impactor tip for both cases was a 16 mm (0.625") steel hemisphere. In spite of the order of magnitude difference in velocity ranges and impactor weights, similar relationships between impact energy, damage size, and residual strength were found. The dependence of the skin compressive strength on damage size agree well with analytical open hole models for composite laminates and may enable the prediction of ultimate performance for the damaged composite, based on visual inspection.

NOMENCLATURE

- a_{oc} : Free parameter in Average Stress Criterion for compression.
- E_x : Young's modulus in x-direction.
- E_y : Young's modulus in y-direction.
- ν_{xy} : Poisson's Ratio.
- G_{xy} : Shear Modulus.
- K_T : Stress Concentration Factor for Infinite Width.
- R : Hole Radius.
- W : Sandwich Panel Width.

Y : Finite Width Correction Factor.

σ_N : Unnotched Strength.

σ_N : Notched Strength for Infinite Width.

σ_N : Notched Strength.

INTRODUCTION

Extensive research on carbon-epoxy laminates has clearly shown that these materials can only accommodate impact energy by developing internal damage which is mainly in the form of a delamination failure mode. The residual compressive strength performance is therefore severely impaired, and may limit the use of these laminates to secondary structures. An additional drawback is that the damage, in most cases, is not detectable by visual examination. Publications which compare low and high-velocity impact response of laminates are rare. Cantwell and Morton (1989) choose a 6 mm (0.236") hemisphere to impact Grafil XA-S/BSL914C laminates with thicknesses varying from 4 to 64 plies. They found that for conditions of low velocity impact, the size and the shape of the target determines its energy absorbing capacity and therefore its impact response. High velocity impact loading induces a localized form of target response and the level of damage incurred does not, therefore, appear to be governed by the areal size of the component. They further concluded that high velocity impact loading by a small projectile is generally more detrimental to the integrity of a composite structure than low-velocity drop-weight impact loading. Moon and Shively (1990) choose a 12.7 mm (0.5") hemisphere to impact 48 ply laminates made of AS4-1806, AS4-934, and IM7-8551-7 prepregs respectively. Their findings were similar to those reported by Cantwell and Morton.

A more comprehensive literature review, on damage tolerance of composites in general was published by Abrate (1991) and by Ishai and Hiel (1992).

Traditionally, sandwich constructions consist of three main parts; two thin, stiff and strong skins separated by a thick, light, and weaker core. The skins are adhesively bonded onto the core to enable load transfer between the components. Composite sandwich construction has been found to be a very efficient way to utilize composite laminates and is therefore used extensively and very successfully in industry. Until recently, the main emphasis was on secondary structural components which require high strength and high stiffness-to-weight ratios. Several damage tolerance studies have been conducted on sandwich constructions having carbon-epoxy skin layers and honeycomb or lightweight foam core. Nevertheless, to the best of the author's knowledge, no work was found that compares the low and high-velocity impact response of

sandwich panels with a structural (syntactic) foam core. This type of material is subsequently referred to as a thick hybrid composite (THC).

Studies on the impact response of THC's have recently been performed (Ishai and Hiel 1992). This paper discusses the relevant details on fabrication, the experimental conditions for low and high-velocity impact, and the inspection and characterization of the impact damage. The relationship between damage size and residual strength is represented by an analytical model. The paper closes with a comparison of the effect of impact energy on the residual strength for both low and high-velocity impacts.

MATERIALS AND FABRICATION

An illustration of the thick hybrid composite is shown in Figure 1a. It consists of the following components:

1. A skin laminate, composed of 18 plies of prepreg (G40-600/5245C) with a (0/+30/-30)_{3s} layup.
2. An external layer for skin protection, composed of two glass fiber fabric 7781/5245 C prepreg layers.
3. A layer of FM300 adhesive.
4. A layer of 7781/5245 C prepreg at +45/-45 orientation.
5. Three layers of syntactic foam (Syntac 350).

The fabrication is as follows: First, the layers of syntactic foam core are cut. Then the different parts, shown in figure 1a, are laid-up into an aluminum mold. After the layup is completed, the mold is closed, vacuum bagged and transferred to a press with heated plattens. The whole assembly is subjected to a 350°F cure cycle after which it is demolded.

It should be noted that this fabrication process has great technological significance since it is also applicable to sandwich constructions with complex geometries because the foam can be cast into any desired shape.

Sandwich beams, with dimensions shown in figure 1b, were cut from the sandwich panel using a diamond tipped bandsaw. The edges were then polished with a diamond coated sander.

IMPACT LOADING

Low velocity Impact

Low velocity impact tests were conducted using a conventional dropweight test rig. An 86 N (19.3 lbs) impactor with a 16 mm (0.625") hemispherical tip was allowed to fall freely from heights ranging from 0.30 m (1

ft) to 2.13 m (7 ft) thereby creating impact velocities ranging from 2.4 m/sec (7.9 ft/sec) to 6 m/sec (19.7 ft/sec). The sandwich beams were simply supported with the distance between the supports being 0.203 m (8").

High Velocity Impact

High velocity impact tests were performed using an airgun. Air with a pressure up to 1.03 Mpa (150 psi) was fed to a chamber. At this point the air was restrained by a plastic diaphragm. When the pressure in the chamber reached a pre-determined value, a small electric current, passed through a piece of resistance wire located at the center of the diaphragm precipitated its rupture and the release of the air. The rapid expansion of the air accelerated a sabot/projectile combination along the length of the 1.79 m (70") barrel. Upon reaching the end of the barrel, the sabot is stopped by a tapered tube (sabot-catcher) allowing the 17 gram (0.04 lbs) projectile to continue free flight and strike the simply supported sandwich beam. The terminal velocities obtained ranged from 40 m/sec (130 ft/sec) to 160 m/sec (525 ft/sec). The velocity was measured by digital clocks which were activated by trip wires located at three locations in the barrel. Both the impactor and the sandwich beams had the same geometry as in the low velocity impact tests.

DAMAGE INSPECTION AND CHARACTERIZATION

The design of the sandwich panels allowed for the extent of damage to be easily differentiated by visual inspection. It was observed that any low or high-speed impact causes a localized damage and delamination of the surface layer of glass-epoxy. The circular delamination is easily visible in both cases and therefore sophisticated NDT equipment is not needed for an initial damage assessment. Cross sectional cutting through the damaged zone was routinely conducted to relate the observed surface- damage and the actual delamination between the skin and the core. Figure 2 indicates that the low velocity impact causes an indentation while the tangential elastic displacements of the contact surfaces cause the formation of a cone crack. Figure 3. is representative for a high-velocity impact with the same energy (and for the same shape of the impactor). The permanent indentation induced by the low speed impactor appears to be deeper than that induced by the high speed impactor at the same impact energy. Additionally, there is substantially more delamination present in the case of high velocity impact. In summary one can state that the impacted skin of a THC at low velocity, as shown in Figure 2. is very similar to the impact damage inflicted on thermoplastic laminates (Starnes and Williams 1983). The impacted skin of a THC at high velocity, as shown in Figure 3. has damage which is very similar to that inflicted on thermoset laminates. It is therefore likely that rate dependence of stiffness and strength in the z-direction needs to be introduced in future mathematical models for THC's.

Further evaluation of the damage mechanism is obtained by relating the damage size to the impact energy as shown in Figure 4. As can be seen, damage caused by both low and high-velocity impacts have a similar dependence on the energy. Final conclusions cannot be formulated at this time, because the damage caused by high velocity impacts has more scatter at the higher impact energies.

Following damage characterization, the sandwich beams were subject to four point bending. The distance between the supports was chosen as 0.33 m (13") with a distance between the loads of 0.076 m (3"). Each THC was loaded with the damaged skin on the compressive side. Strength was defined as the Skin Stress at Failure (SSF).

RESIDUAL STRENGTH

The low and high-velocity impact damage was localized, and is therefore expected to have only a limited effect on the beam stiffness. They act, however, as stress raisers and can therefore have a significant effect on laminate strength. This is evident from figure 5, where the residual strength is plotted as a function of damage diameter. Again it can be seen that there is basically no difference between reduction in strength due to low and high-velocity impacts. The solid curve was obtained by using the Whitney-Nuismer (1974) average stress failure criterion which leads to the following Equation:

$$\sigma_N = \frac{\sigma_N^{\infty}}{Y(2R/W)}$$

which states that the notched strength (which is experimentally measurable) can be obtained by dividing the strength of an infinitely wide laminate by a correction factor Y , which is can be calculated as follows;

$$Y(2R/W) = \frac{2 + \left(1 - \frac{2R}{W}\right)^3}{3 \left(1 - \frac{2R}{W}\right)}$$

strictly speaking, this equation is only correct for isotropic laminates and therefore Y is called the "isotropic finite width correction factor". Gillespie et al (1988) have shown nevertheless that the above expression is applicable to orthotropic laminates for d/W values smaller than .25, which was the case in this investigation.

According to Whitney and Nuismer (1974) the notched strength of an infinitely wide orthotropic plate is related to the unnotched strength by the following equation;

$$\sigma_N^{\infty} = \frac{2\sigma_0(1-\xi)}{[2-\xi^2-\xi^3+(K_T^{\infty}-3)(\xi^6-\xi^8)]}$$

with

$$\xi = \frac{R}{R+a_{oc}}$$

and

$$K_T^{\infty} = 1 + \left\{ 2 \left[\left(\frac{E_x}{E_y} \right)^{0.5} - \nu_{xy} + \frac{E_x}{2G_{xy}} \right] \right\}^{0.5}$$

The equations were originally used to predict the variation of tensile strength due to a through the thickness hole (or notch) in a multi-ply laminate. The quantity a_{oc} was introduced to represent a characteristic damage zone in the highly stressed region adjacent to the hole. The distance is used as a free parameter to be determined by fitting experimental data assuming an average stress over the damage zone. This criterion has been extended to include compression loaded laminates by Nuismer and Labor (1979).

Our basic assumption in using the described analytical approach to THC's, is that the impact damages material over a radius R , and that this material no longer participates in the load transfer process within the laminate. Therefore the damaged material can effectively be thought of as nonexistent and be considered as a hole with radius R . The parameter a_{oc} for the present data was found to be 6.09 mm (0.24"), which is very close to the result obtained by Nuismer and Labor (1979) on a carbon epoxy laminate.

Figure 6 relates the residual strength to the impact energy, and shows that both the low and high-velocity data can be merged onto a single master curve. It may therefore be concluded that impact energy is the single most important factor to control residual strength reduction of structural sandwich panels with interleaved core (provided the same impactor tip is used).

CONCLUSIONS

- o Damage size was found to be similar for both low and high velocity impacts having the same energy.
- o Damage microstructure was found to resemble thermoplastic materials at low impact velocity and thermoset laminates at high impact velocity.

- o Reduction in residual strength is directly controlled by the impact energy, while impact velocity plays a minor role.
- o The Whitney-Nuismer average stress criterion, for open hole laminates, provides an appropriate presentation of the experimental data which relates damage size to residual strength.

ACKNOWLEDGMENT

The authors express their appreciation to Michael Luft, Howard Nelson and Dave Chappell of the Test Engineering and Analysis Branch at NASA Ames Research Center for their support and encouragement. They also acknowledge the substantial manufacturing expertise dedicated to this project by Paul Scharmen of the Ames Modelshop.

REFERENCES

- Abrate, S., 1991, "Impact on Laminated Composite Materials," *Applied Mechanics Reviews*, vol 44, #4, April 1991, pp 155-190.
- Cantwell, W.J., and Morton J., 1989 "Comparison of the Low and High Velocity Impact Response of Sandwich Panels," *Composites*, Vol. 20, Number 6, pp 545-551.
- Freeguard, G.F., and Marshall, D., 1980, "Bullet-Resistant glass- A review of product and process technology," *Composites*, January, pp 25-32.
- Gillespie, J.W., and Carllson, L.A., (1988) "Influence of Finite Width on Nothced Laminate Strength Predictions," *Composites Science and Technology*, 32.
- Hiel, C., and Ishai, O., 1991 "Low- and High-Velocity Impact Response of Sandwich Panels with Syntactic Foam Core," *Proceedings ASME Winter Annual Meeting*, Atlanta, Ga Dec 1-6.
- Ishai, O. and Hiel, C.C., 1992, "Damage Tolerance of Composite Sandwich Panels with Interleaved Foam Core," *Journal of Composites Technology and Research*, Vol 14, #3 ,Fall 1992
- Masters, J.E., 1987, "Correlation of Impact and Delamination Resistance in Interleaved Laminates," *Proceedings of the Sixth International Conference on Composite Materials*, Eds. F.L. Matthews et al., Vol 3, pp 3.96-3.107.
- Moon, D., and Shively, J.H., 1990, "Towards a Unified Method of Causing Impact Damage in Thick Laminated Composites," *Proceedings of the 35-th International SAMPE symposium*.

Nuismer, R.J., and Labor, J.D., 1979, "Applications of the Average Stress Failure Criterion: Part II-Compression," J. Composite Materials, 13: 49-60,.

Starnes, J.H., and Williams, J.G., "Failure Characteristics of Graphite-Epoxy Structural Components Loaded in Compression," Mechanics of Composite Materials-Recent Advances- Hashin, Z., and Herakovich, C.T., Pergamon Press, 1983, pp 283-306

Whitney, J.M. and R.J. Nuismer, 1974, "Stress Fracture Criteria for Laminated Composites Containing Stress Concentrations," J. Composite Materials, vol 8, p.253.

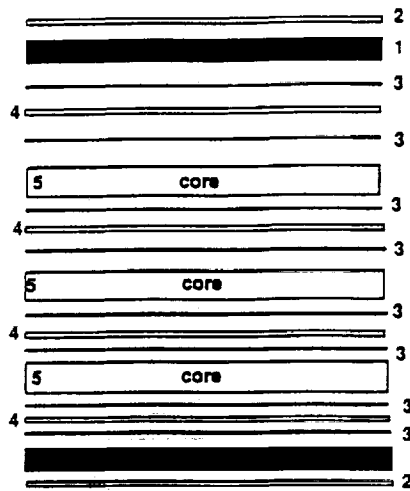


Fig. 1(a) Identification of materials in interleaved sandwich panels

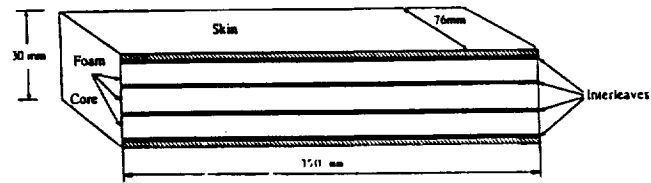


Fig. 1(b) Principal dimensions of interleaved beam



Fig. 2 Low-velocity impact damage: cross-sectional view

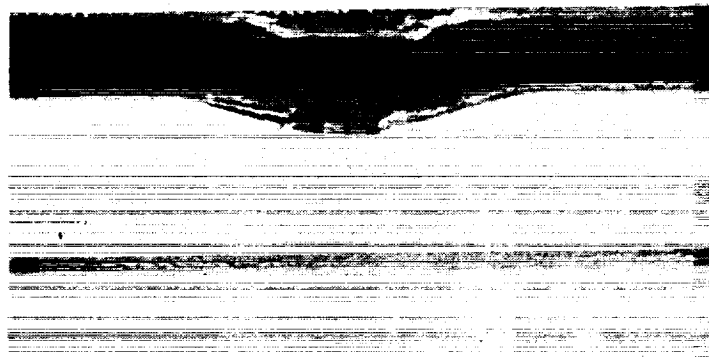


Fig. 3 High-velocity impact damage: cross-sectional view

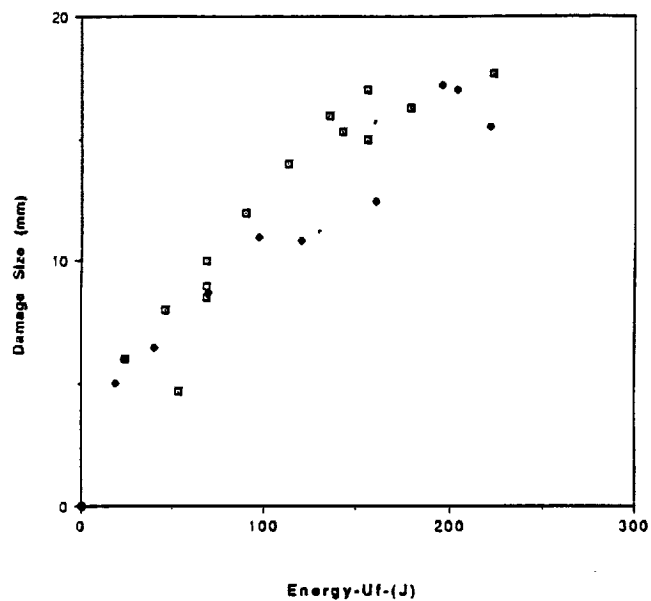


Fig. 4 Dependence of damage size on impact energy
 ■ low velocity impact
 ● high velocity impact

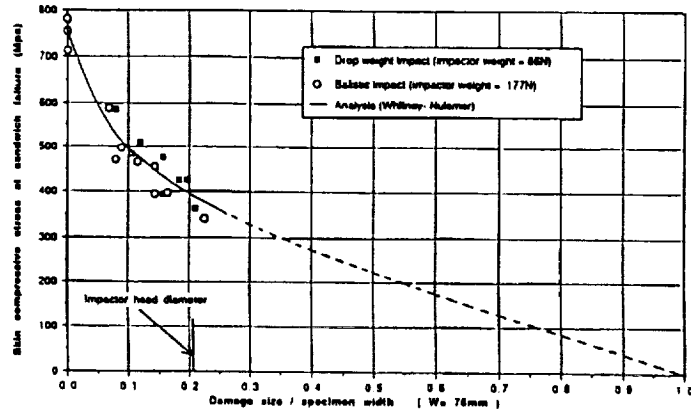


Fig. 5 Dependence of residual strength on damage size (normalized by specimen width)

- low velocity impact
- high velocity impact

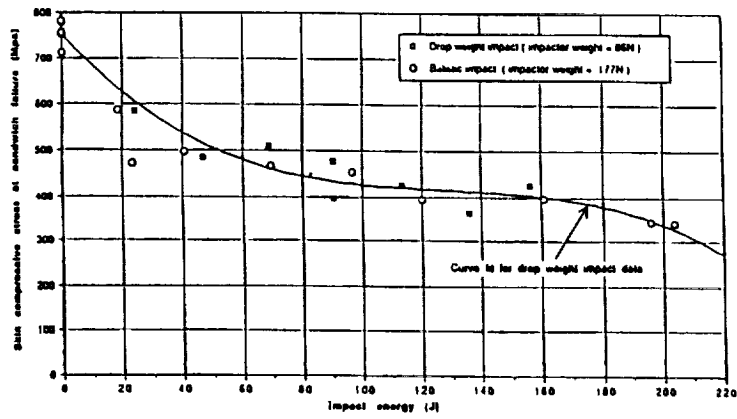


Fig. 6 Dependence of residual strength on impact energy

- low velocity impact
- high velocity impact

Ori Ishai¹ and Clement Hiel²

Damage Tolerance of a Composite Sandwich with Interleaved Foam Core

REFERENCE: Ishai, O. and Hiel, C., "Damage Tolerance of a Composite Sandwich with Interleaved Foam Core," *Journal of Composites Technology & Research*, JCTRER, Vol. 14, No. 3, Fall 1992, pp. 155-168.

ABSTRACT: A composite sandwich panel consisting of carbon fiber-reinforced plastic (CFRP) skins and a syntactic foam core was selected as an appropriate structural concept for the design of wind tunnel compressor blades. Interleaving of the core with tough interlayers was done to prevent core cracking and improve damage tolerance of the sandwich. Simply supported sandwich beam specimens were subjected to low-velocity, drop-weight impacts as well as high-velocity, ballistic impacts. The performance of the interleaved core sandwich panels was characterized by localized skin damage and minor cracking of the core. Residual compressive strength (RCS) of the skin, which was derived from flexural test, shows the expected trend of decreasing with increasing size of the damage, impact energy, and velocity. In the case of skin damage, RCS values of around 50% of the virgin interleaved reference were obtained at the upper impact energy range. Based on the similarity between low velocity and ballistic impact effects, it was concluded that impact energy is the main variable controlling damage and residual strength, where as velocity plays a minor role. The superiority (in damage tolerance) of the composite sandwich with interleaved foam core, as compared with its plain version, is well established. This is attributable to the toughening effect of the interlayers which serve the dual role of crack arrestor and energy absorber of the impact loading.

KEYWORDS: damage, damage tolerance, impact, ballistic impact, impact velocity, impact energy, sandwich beam, interleaving, syntactic foam, residual strength, carbon fiber-reinforced foam

Nomenclature

BVD	Barely visible damage
CFRP	Carbon fiber-reinforced plastic
CTE	Coefficient of thermal expansion
DTC	Damage tolerance characteristics
DTE	Damage tolerance evaluation
FRP	Fiber-reinforced plastics
GFRP	Glass fiber-reinforced plastic
HC	Honeycomb core

¹Presently, visiting scientist, NASA Ames Research Center, Mail Stop 213-3, Moffett Field, CA 94035; permanently, professor, Technion-Israel Institute of Technology, Haifa, Israel.

²Principle investigator, Composite Material Research Program, NASA Ames Research Center, Mail Stop 213-3, Moffett Field, CA 94035.

RT	Room temperature conditions
RCS	Residual compressive strength
SSSF	Skin maximum compressive stress at sandwich failure
b	Sandwich width
d_i	Impactor diameter
E_{11}, E_{22}	Lamina longitudinal and transverse elastic moduli, respectively
F_{1t}, F_{2t}	Lamina longitudinal and transverse tensile strength, respectively
F_{1c}, F_{2c}	Lamina longitudinal and transverse compressive strength, respectively
F_6	Lamina in-plane shear strength
G_{12}	Lamina in-plane shear modulus
g	Constant of gravity
H	Drop-weight height
h	Sandwich thickness
L_0	Sandwich span
t	Skin thickness
t_0	Ply thickness
W_i	Impactor weight
α_1, α_2	Lamina longitudinal and transverse CTE, respectively
ν_{12}	Lamina longitudinal Poisson's ratio

Introduction

Composite materials are considered to be good candidates for replacing metals in helicopter and compressor blades applications. This is due to their superior mechanical properties such as: high strength and stiffness per unit weight, long fatigue life, durability, and better damage tolerance characteristics (DTC). The last advantage has been shown to be of major importance by past failures of aluminum wind tunnel blades. NASA Ames promoted a research and development (R&D) project to provide input data for comparing composites and aluminum design alternatives for wind tunnel compressor rotor blades. A composite sandwich structure composed of CFRP skins and foam core was chosen as an appropriate concept. The effect of impact on damage and consequential residual strength were selected as a major subject for investigation. At an early stage of the research it was found that an elevated-temperature-cured sandwich, with a full depth plain syntactic foam, was highly sensitive to impact loading. This was manifested by extensive cracking of the core and poor residual strength. To reduce this effect, the core was toughened by interleaving with adhesive and glass/epoxy interlayers.

The main objective of the present investigation was to provide experimental data for damage tolerance evaluation (DTE) of this complex composite sandwich system.

Damage Tolerance Methodology for Structural Composite Laminates

Most investigations dealing with DTE are aimed at three main objectives:

- The assessment of structural performance under static or cyclic loads or both as well as survivability of structural elements, which were previously damaged by accidental impact.
- To provide guidelines and allowables for design and quality assurance of composite structures which are likely to sustain impact damage and where DTE has to be considered.
- Ranking, for material selection purpose, of different composite systems based on their response to impact and their residual structural performance.

The first issue is of major concern for aircraft industries and certification authorities. For this purpose, some specifications and requirements based on DTE have been proposed [1,2]. These assessments are mainly related to critical levels of impact energy and damage size. Another DTE classification is defined as "barely visible damage" (BVD) threshold. Data on carbon-epoxy laminates indicate that at BVD level, compression strength after impact may decrease to as low as 40% of the undamaged reference strength. The respective level of residual compressive strain seems, nowadays, to be the accepted allowable design limit for high performance carbon-epoxy composites in structural aircraft applications. Most investigations that are concerned with material selection are based on several attempts to standardize DTE testing methods [3,4]. This effort is essential because of the high sensitivity of the composite to the impact test variables such as: the impactor diameter, the specimen geometry, and its boundary conditions [5-7].

The effect of impact velocity has also been considered. There is a clear distinction between the low velocity drop-weight test and the high velocity (ballistic) test as a result of their probable different effects on damage characteristics [8-10]. The effect of material composition on DTE can only be evaluated by keeping a uniform test method. Several investigations that have used the clamped plate [8,11,12] or narrow beam configurations [13] have indicated a strong effect of different material parameters on DTE, namely: variation in layer stacking sequence, using thermoplastic rather than thermoset resin as a matrix, interleaving the laminate with tougher plies, and so forth. During the last decade, most of the publications on DTE were limited to composite laminates. Studies on the effect of impact on damage and residual performance of substructural elements such as sandwich panels have been less frequent, possibly as a result of the numerous parameters and the complexity involved.

Damage Tolerance Evaluation of Composite Sandwich Panels

Composite skins in sandwich panels subjected to flexural impact behave entirely different than plate laminates mainly for the following two reasons. First, the skin is under plane axial loads when the sandwich is under flexure, hence, interlaminar shear stresses are confined mainly to the local impacted zone. Second, the core provides a relatively soft substrate which locally

may absorb the impact energy. The weak link in sandwiches in many cases is the core material, which may fail by shear or tensile stresses induced under flexural impact. Most of the publications on this topic deal with sandwiches composed of honeycomb core and CFRP skins. Similar to the DTE of laminates, the evaluation of sandwiches is treated at three levels, namely: the effect of fabrication flaws, artificial flaws, and impact damage.

The following types of flaws as a result of fabrication may be detected: cracks in the core caused by thermal curing stresses, partial separations at bonded interfaces in the core and between core and skins, skin transverse cracking, and delaminations. Core flaws were found to affect sandwich performance as a result of the reduction in its shear strength and modulus [14,15]. Interfacial separation also has a significant effect on strength above critical debonding length and depends on skin configuration [16]. To enable the evaluation and prediction of the effects of flaw size and location on the composite sandwich performance, artificial flaws are inserted into the sandwich structure. Information from these studies may lead to the definition of flaw criticality and the related strength which is essential for sandwich design and quality assurance. In most cases, artificial flaws are embedded within one of the skins in a sandwich which is subjected to flexure or compressive loading up to failure [17,18]. Analytical models are based, in many cases, on the sublaminar buckling mechanism of delaminated composites [19,20]. It has been claimed that damage caused by low velocity impact has the most severe effect on laminate and sandwich performance [1]. Tests conducted on CFRP skin and honeycomb (HC) core have indicated that, at BVD level and above, damage is characterized by local fiber breakage and delamination of the impacted skin [21]. Residual strength in most cases is below 50% of the nondamaged reference. Analytical model predictions gave more conservative results than experimental data. It was concluded, in other investigations, that impact energy to failure increases with skin thickness and its rigidity [22]. Increasing honeycomb density tends to improve damage tolerance, but cell dimension has only a minor effect.

Several investigations dealt with the effect of ballistic impact when a small diameter impactor was used [23-25]. In most cases, the damage was characterized by combined fiber fractures and local internal delaminations. This failure mode may be modeled as a hole through the skin. Predictions of residual strength, based on this model, are in good agreement with experimental findings [26]. Investigation into the effect of cyclic compressive loading [25,27] has indicated that even at BVD level, fatigue life may be reduced as a result of propagation of delaminations and interfacial separations which were formed during impact.

Several investigations deal with the effect of impact on sandwiches with different combinations of skin and core materials such as: aluminum, glass-phenolic and Nomex[®] honeycombs, three-dimensional (3-D) fabric, and Rohacell[®] foam. Skins, in most cases, are composed of graphite-epoxy [28-31]. Tests have shown that by proper selection of core material, adhesive, and hybridization with tougher fibers, the mechanical properties of the sandwich may be varied widely with corresponding improvement in impact energy absorption. Recently, attention has shifted toward attempting to understand and predict the behavior under impact of basic structural composite elements which are mainly used in aircraft applications [32,33]. Such studies try to establish a more standardized DTE approach for structures and provide guidelines for improving the damage tolerance by proper selection of materials and composite layup variable.

The Effect of Interleaving

During the last decade, many efforts have been dedicated toward improving fracture toughness and damage tolerance of advanced composites with brittle epoxy matrices designated for elevated temperature applications. A comprehensive review of this topic [34] summarizes the different techniques, test methods, and properties of toughened composites. One of the most promising approaches was the interleaving of the carbon-epoxy laminates by softer and tougher materials such as adhesive films. It was found that interleaving may reduce interlaminar stresses at critical locations [35], hereby significantly increasing the interlaminar fracture toughness, decreasing and controlling impact damage, and improving RCS [13,36,37]. This approach was extended to include different interleaving materials such as thermoplastic films and hybridization using tougher FRP interlayers [38-40]. It was also used successfully at the structural element level [41,42]. To the best knowledge of the authors, the interleaving method has not been used in conjunction with syntactic foams. While this is probably a result of the limited application to date of these foams in high performance sandwich structures, it is, however, reasonable to assume that the interleaving technique may significantly improve impact damaging effect and subsequent residual strength of sandwiches composed of these core materials.

Concluding Remarks

Based on the above literature review and information on mechanics of sandwich structures, the following general comments may be concluded in relevance with the present investigation:

- The composite skin is the backbone of the sandwich structure and provides its strength and stiffness.
- The main function of the core is to support the skins to avoid local buckling and to absorb energy as a result of local impact. It must also possess enough strength and stiffness for the transfer of shear and tensile stresses under flexural loading.
- Syntactic foams, which are composed of epoxy resin reinforced with glass microballoons, have higher density than other foams and HC cores. They possess, however, better strength and stiffness characteristics as required for high performance structural sandwich applications.
- Syntactic foams for elevated temperature applications (350°F [176.6°C]) may be cracked under impact loading because of their relative high brittleness and induced curing tensile stresses due to their high coefficient of thermal expansion. Interleaving techniques, which have been proven successful for composite laminates, offer promise for improving damage tolerance characteristics of syntactic foam sandwich structures.

Objectives

The objectives of the present research are as follows:

- Study the effect of impact loading on damage and subsequent residual strength of composite sandwiches with syntactic foam cores.
- Develop a database for interleaved core sandwich structure taking into account damage tolerance considerations.
- Investigate the effect of core composition parameters on DTC to provide design guidelines for optimizing sandwich postimpact structural performance.

Materials and Specimens

Sandwich structures are usually composed of three main components, namely, skins, core, and an adhesive which bonds them together. In the present case, a fourth phase, the interleaved layers, is added. All of the constituent materials for the above components were cured at 177°C (350°F) and are designated to be used under service conditions of up to 122°C (250°F).

Constituent Materials

The structural **skins** were fabricated from unidirectional carbon fiber-reinforced bismaleimide (CFRP) prepreg tapes (Rigidite G40-600/5245C) supplied by BASF. Each skin consisted of 18 plies (average ply thickness of 0.14 mm) with the following layup: $(0/+30/-30)_s$. Two layers of BASF glass fabric-reinforced epoxy (GFRP) prepreps (7781/5245C) were added for external protection of each skin. The **core** was made of prefabricated solid syntactic foam (Syntac 350) supplied by Grace Syntactic. It is composed of epoxy resin filled with glass microballoons having the density of about 0.6g/cm³. The **adhesive** used was FM300 prepreg film made by American Cyanamid Corp. The **interleaved** phases consisted of one ply of glass fabric prepreg oriented at $\pm 45^\circ$ to the beam axis embedded between two plies of adhesive film.

Sandwich Specimens

A typical sandwich specimen configuration with interleaved core is illustrated in Fig. 1. It consists of two CFRP skins with the GFRP fabric coating and three foam core layers which are bonded together with the skins by four interleaves. In the case of plain core reference specimens, the skins were bonded to the core with adhesive film (FM300). Sandwich panels were fabricated by cocuring of the skin plies and interleave prepreps together with the solid core pieces by means of a press-molding process (under pressure of about 6 atm). Two types of specimens were cut from the cured panels as follows:

- Long beams of about 350 by 76 by 30 mm for residual strength tests.
- Short beams of about 210 by 76 by 30 mm for cross-sectional damage assessment.

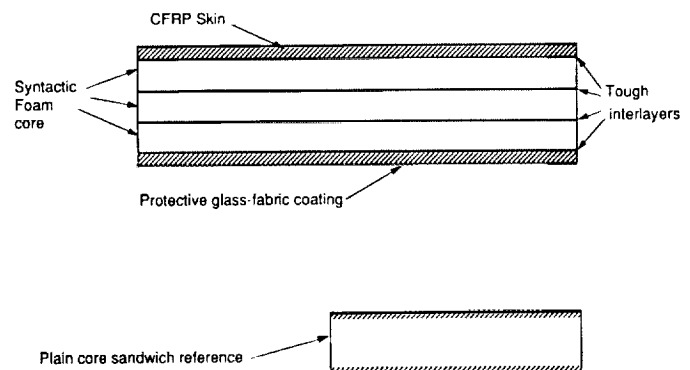


FIG. 1—Typical configuration of composite sandwich with interleaved core and plain core sandwich reference.

After rough cutting with a carbide-coated saw, the specimens' edges were machined and polished under water by means of a diamond powder-coated disk to attain smooth and parallel surfaces.

Characteristics of Sandwich Constituents

The basic mechanical properties of the cured, unidirectional CFRP lamina, the GFRP fabric, the syntactic foam, and the adhesive layers are given in Table 1. They are designated for the cured state at room temperature (RT) dry condition. Most of the constituents' data were obtained from the available literature and supplier information. The properties of the syntactic foam were obtained independently following ASTM test standards (ASTM Test for Tensile Properties of Plastics [D 638], ASTM Test for Flatwise Compressive Strength of Sandwich Cores [C 365], and ASTM Test for Shear Properties in Flatwise Plane of Flat Sandwich Constructions or Sandwich Cores [C 273]). Most of the CFRP skin properties were computed based on the respective lamina inputs, using composite laminate analysis, except for the compressive strength (F_{1c}) and the coefficients of thermal expansion (α_1, α_2) which were obtained experimentally.

Test Procedure

A flow chart of the research program and test procedure is shown in Fig. 2. Accordingly, two identical series of specimens were subjected to low velocity and ballistic impact loading. After visual damage assessment, these specimens were loaded in flexure to failure for residual strength determination. Damage tolerance characteristics of interleaved and plain core reference sandwich configurations were evaluated based on the relationships between impact variables and damage characteristics and between these parameters and residual strength.

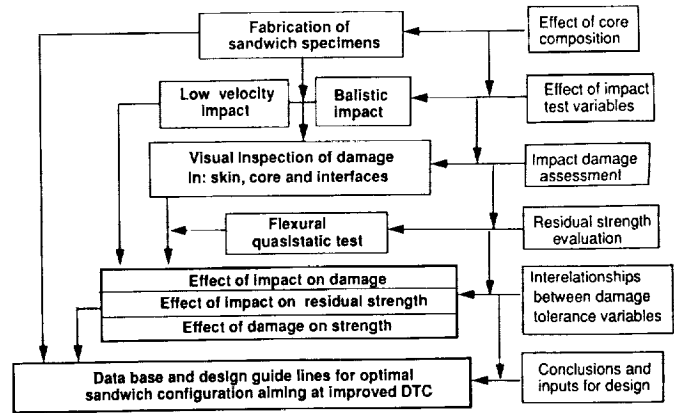


FIG. 2—Scheme of research program and test procedure.

Impact Testing

Two types of impact tests were designated to represent the range of impact events which may occur to compressor blades during installation, maintenance, and wind tunnel operation. They are commonly defined as low velocity (drop-weight test) and high velocity (ballistic test), respectively. An illustration and basic specifications of these tests for the present investigation are shown in Fig. 3. There is a large difference in impact velocity and impactor weight between the two tests; however, to get a reliable comparison between low and high velocity tests the impactor head geometry was kept identical in the two cases.

Drop-Weight Impact Test

The instrumented impact system comprises of a Impact 66 test machine made by Monterey Research Laboratories. The maxi-

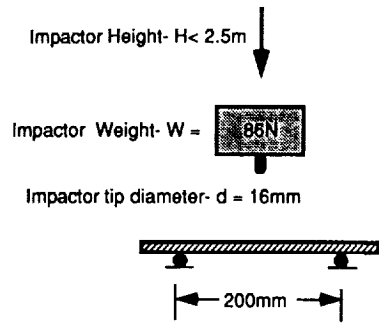
TABLE 1—Sandwich constituents properties.

UNITS	ELASTIC PROPERTIES				STRENGTH PROPERTIES					C.T.E		Thick. (mm)
	GPa				MPa					$C^{-1} \times 10^{-6}$		
MATERIAL	E11	E22	G12	ν_{12}	F1t	F1c	F2t	F2c	F6	α_1	α_2	10
CFRP G40-600 5245C	170	11.8	5.2	.33	2070	1380	75	251	102	-.3	28	.14
GFRP Fabric 7781 5245C	30.3	30.3	5.4	.17	374	560	374	560	99	9.9	9.9	.24
Syntactic Foam 350C	2.26	2.26	.84	.31	27	54.6	27	54.6	25	48*	48*	
Adhesive FM300 .08psf	2.45	2.45	.88	.38	53	98	53	98	35	77	77	.26
CFRP Skin (0/30/-30) _{3s} (**)	97.2	14.8	24.5	1.21	936	660	70	289	153	-3.3*	15.1*	2.52

*) Coefficient of Thermal Expansion Values were determined experimentally at temperature range of 20-120°C

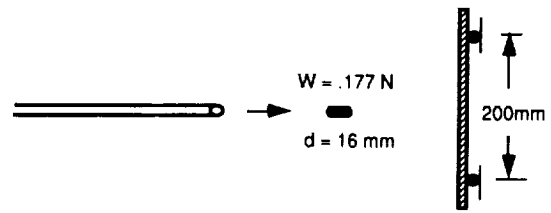
***) Most of CFRP skin properties were computed based on the respective lamina inputs, except α_1 , α_2 and F_{1c} which were derived experimentally.

Low velocity, (Drop weight) set-up



Velocity range : up to 6 m/sec
Energy range : up to 160 J

High velocity (ballistic), Air-gun set-up



Velocity range : up to 160 m/sec
Energy range : up to 220 J

FIG. 3—Illustration of setups for two types of impact tests.

mum tower height is about 3.0 m. The impactor comprises of a 16-mm-diameter hemispherical tip (hardened steel) attached to a rigid base with the assembly weighing 86 N. The impactor is raised to the required height by the hydraulic system and released pneumatically. Its rebound is arrested automatically by a braking system to insure a single-impact event. During the fall, the impactor is guided by two lubricated circular columns. To account for the friction during falling, the exact values of impact variables was derived experimentally. The velocity was determined optically by measuring the elapsed time between two photo cells. The actual maximum velocity and the derived kinetic energy just before the collision are plotted as functions of the drop height in Fig. 4 in comparison with the respective predicted curves. The

lower values of the measured velocity and energy variables as compared to the predicted ones are attributed mainly to frictional resistance to the falling weight. The average calculated drop acceleration was about 0.88g. The dynamic response of the system during the impact process was monitored by a dynamic signal analyzer Type 3562A made by Hewlett Packard using accelerometer Type 2252 made by Endevco which was attached to the top of the impactor. Most of the impacted sandwich beam specimens were simply supported on two rollers having a span of about 200 mm. Typical acceleration and the integrated velocity versus time responses recorded during impact of interleaved and plain core sandwiches are shown in Figs. 5 and 6, respectively. The acceleration response in Fig. 5, which is typical for the

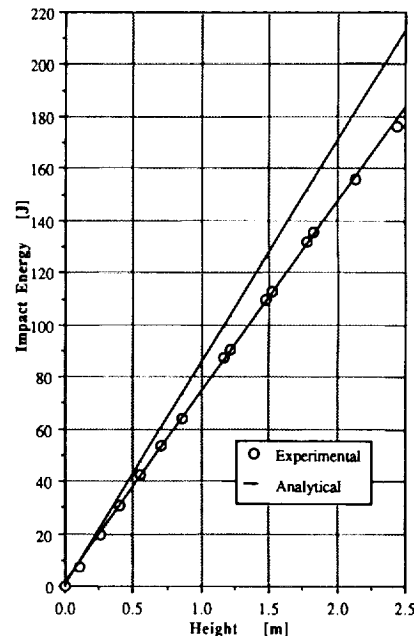
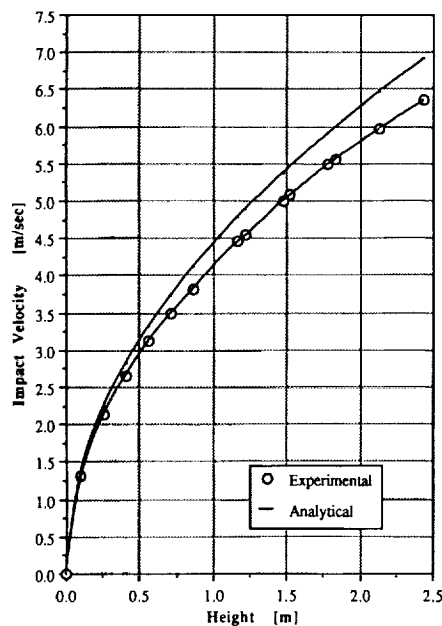


FIG. 4—Calibration curves of impact variables as function of drop-weight height.

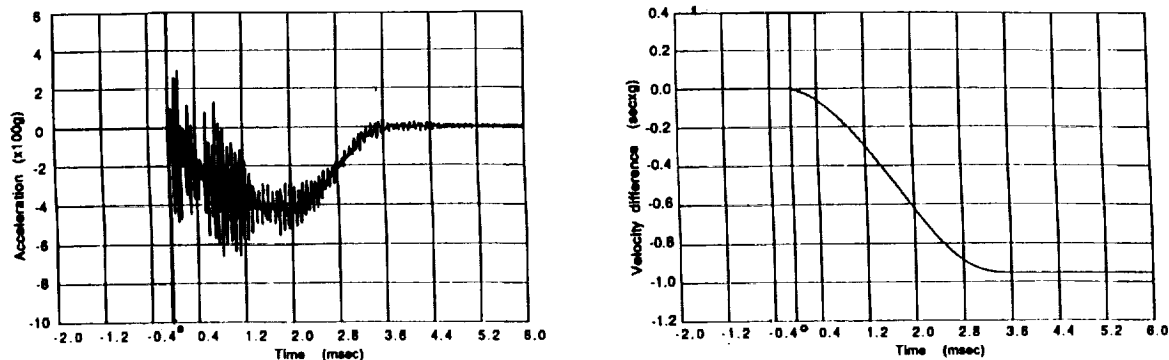


FIG. 5—Typical acceleration and velocity response curves for interleaved core sandwich. Recorded during low velocity impact test (input energy: 156 J) (skin damage only).

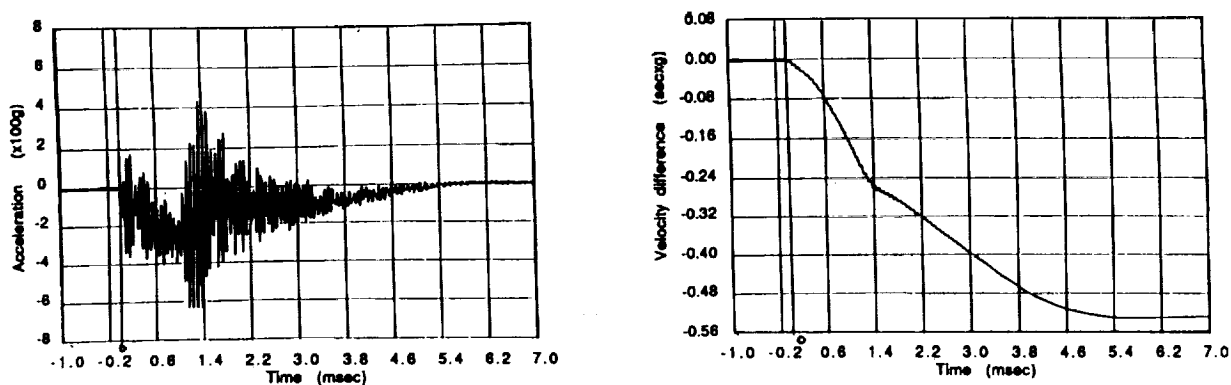


FIG. 6—Typical acceleration and velocity response curves for plain core sandwich. Recorded during low velocity impact test (input energy: 68.7J) (core damage mainly).

noncracked interleaved core sandwich, shows a trend towards a minimum (or maximum deceleration) which is not easy to define quantitatively as a result of the graph fluctuations. The velocity curve, which is obtained by integration of the acceleration graph, is smooth and continuous and allows precise determination of the minimum acceleration from its extreme slope. The difference between the input impactor velocity and response velocity is used for computation of energy loss as a result of energy absorbed, mainly by the skin local damage during the impact process. On the other hand, the response of the plain core sandwich to the impact is different (Fig. 6). It is characterized by a highly scattered acceleration graph with no trend at all and a discontinuous velocity curve attributable to the cracking of the noninterleaved core during impact. Here, the lower upward velocity after impact (as compared with the control specimens with the interleaved core) indicates higher energy loss, mainly due to the failure process in the sandwich core.

High Velocity (Ballistic) Impact Test

Ballistic tests were conducted by using an air-gun device. Air pressure (up to 1.03 MPa) was fed to a chamber in which it was restrained by a thin plastic diaphragm. At a predetermined pressure level, the diaphragm was ruptured by electrical heating and

the air was released. The abrupt air expansion accelerated a sabot/impactor combination along the 1.79-m tapered barrel which caught the sabot at its end. After a short free flight, the 17-g impactor collides with a simply supported sandwich beam specimen. The terminal velocities obtained, which were controlled by the air pressure, ranged from 40 to 160 m/s. The velocity was measured by digital clocks activated by trip wires located at three positions close to the barrel edge. Both the impactor and the sandwich beam had the same composition and geometry as those used for the drop-weight, low velocity impact test.

Impact Damage Characterization

After impact loading, each specimen was inspected visually and the external dimensions of the damage were measured, namely: the damage size and its depth. In most cases, the damage shape was close to circular and the average diameter was considered to be a measure of its size. Maximum damage depth was measured by a special indicator to an accuracy of 0.01 mm. Different specimens, representative of the overall impact range, were sectioned through the damage center for internal inspection of the damage sandwich. Typical photographs of external and internal damage surfaces for the interleaved specimens are shown in Figs. 7 and 8 and will be discussed later.

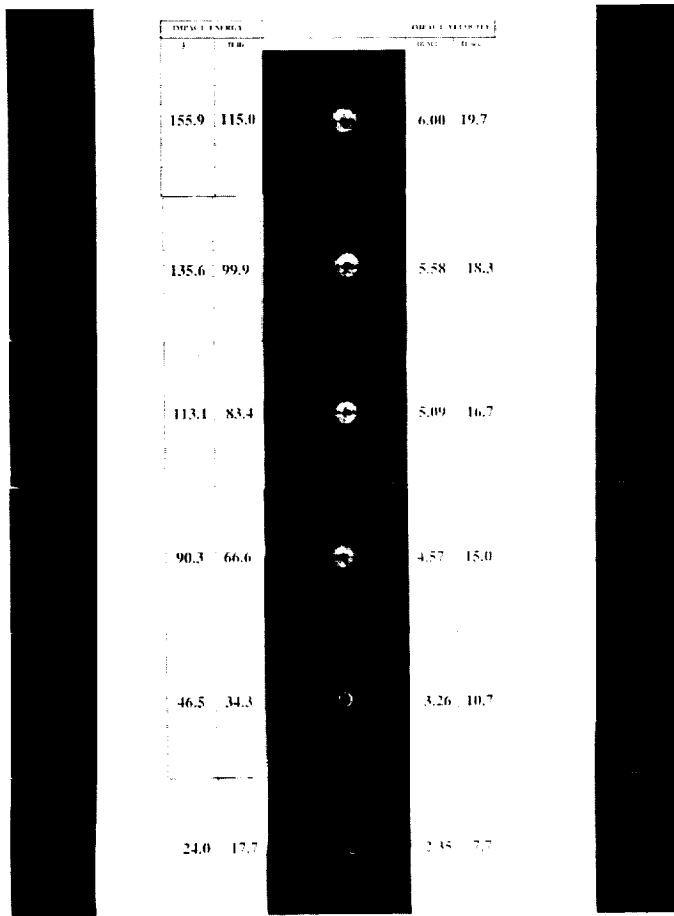


FIG. 7—External (top) view of damage for interleaved core sandwich specimens subjected to different low velocity impact energy levels.

IMPACT DAMAGE IN COMPOSITE SANDWICH PANELS WITH INTERLEAVED FOAM CORE (CROSS-SECTION VIEW)

IMPACT ENERGY		CROSS-SECTION VIEW	IMPACT VELOCITY	
	ft.lb		m/sec	ft/sec
155.9	115.0		6.00	19.7
113.1	83.4		5.09	16.7
68.7	50.7		3.96	13.0
46.5	34.3		3.26	10.7
24.0	17.7		2.35	7.7

FIG. 8—Internal (cross-sectional) view of damage for interleaved core sandwich specimens subjected to different low velocity impact energy levels.

Residual Strength Testing

Following external damage inspection, the specimens were loaded to ultimate failure in four-point flexure using an MTS test system. In all cases, the sandwich was placed so as to load the damaged skin in compression. Constant cross-head speed of 1.84 mm/min was maintained during the test. An illustrative description of the flexural system is shown in Fig. 9. The relevant values of the skin compressive stress at sandwich failure (SSSF) and the core shear stress at sandwich failure (CSSF) were derived from the ultimate load P_u value based on the simplified sandwich beam formulations. A classical sandwich analysis was used for the derivation of stress formulation given in Fig. 9. It is justified due to the high stiffness ratio between the CFRP skin and the interleaved core (above 30).

Skin stress at skin failure (SSSF) is the maximum effective stress acting on the upper side of the skin laminate cross section at failure. The SSSF value represents the residual compressive strength (RCS) of the damaged skin laminate and the residual strength of the sandwich. The skin laminate is treated here macroscopically as a quasi-homogeneous material under uniaxial stress loading. The load-deflection relationship was linear to failure which was catastrophic and brittle. Hence, maximum stress criterion was found to be adequate.

Test Results

Test results and their evaluation are involved with several variables and characteristics which may be classified into three main groups, namely: impact variables, damage characteristics, and residual strength variables. A detailed list of these variables is given in Fig. 10.

Impact Damage Assessment

The protective glass fabric-epoxy layers on the external skin surfaces were found to be highly sensitive to the impact loading which left clear imprints whose dimensions varied with the impact magnitude (see Fig. 7). The boundaries of these imprints seems to be dictated by the contact surface between the impactor tip and the specimen. The dimensions of internal interfacial debonded area measured from the cross-sectioned specimens (Fig. 8) were found to match approximately the respective external imprint sizes at all impact levels. It was concluded that this type of coating may provide an excellent tool for impact damage inspection and assessment in a real structure, where skin damage is the predominant failure mode. In all cases, tested skin impact damage was confined to a well-defined local zone which was almost circular. The predominant failure modes were transverse cracking and delaminations which did not propagate beyond the externally defined damage zone (see Fig. 11). In the case of the specimens with interleaved core, initiation of core cracking originating from the skin damage zone could be detected (Fig. 11). This cracking process seems to be arrested by the internal interleaves which were slightly damaged at high impact levels. These findings demonstrate the effectiveness of the interleaving process for either preventing or delaying core failure. In the case of the plain (noninterleaved) core specimens, cracks developed through the core depth which were activated by the combined action of tensile curing stresses and shear stresses induced by the flexural impact. A typical pattern of such cracking is shown in

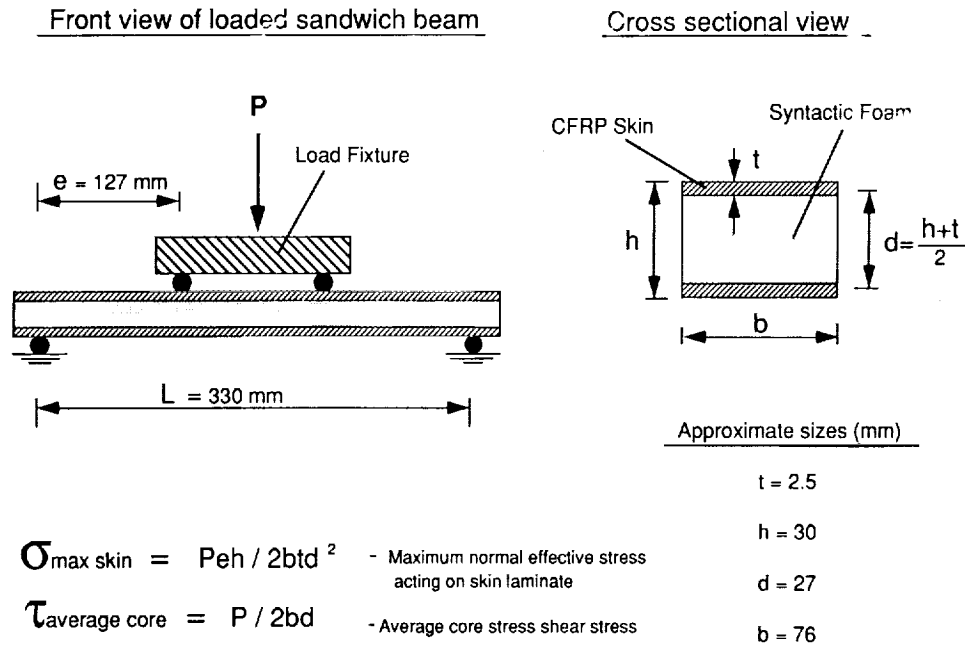


FIG. 9—Flexural test setup and formulation for derivation of residual strength.

Impact Variable

- Impact Energy (input) U_i - Derived from experimental energy plot (fig. 4)
- Impact Velocity (input) V_i - Derived from experimental velocity plot (fig. 4)
- Energy Loss (response) ΔU - Computed from input and output velocity difference

Damage Characteristics

- Damage Size (diameter) D_s - Average diameter of visual external damage (fig. 7)
- Damage Depth d - Maximum depth of skin damage crater (fig. 11)
- Damage Area $A_d = \pi D_s^2/4$
- Failure modes (Skin, Core or Interfacial)

Residual Strength Variables

- Skin max. compressive stress at skin failure SSSF
- Skin max. compressive stress at core failure SSCF
- Core max. shear stress at skin failure CSSF
- Core max. shear stress at core failure CSCF

FIG. 10—List of test variables.

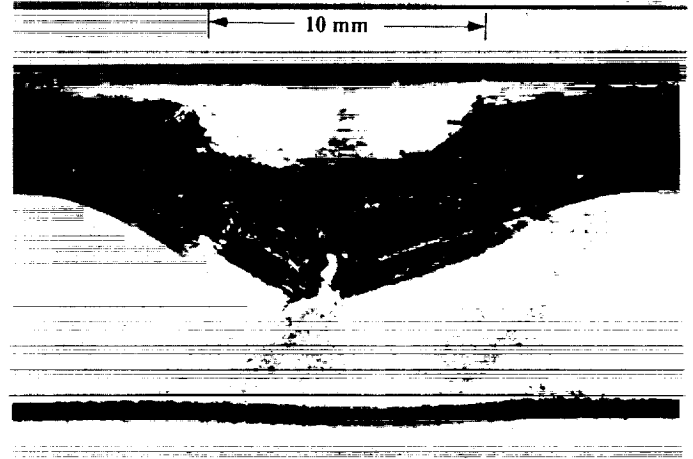


FIG. 11—Typical cross-sectional view of low velocity impact damage for composite sandwich with interleaved syntactic foam core (impact velocity: 6m/s; impact energy: 156 J).

Figs. 12 and 13 for the plain core version as compared with its interleaved counterpart.

The Effect of Impact Variables on Damage Characteristics

In general, three parameters may be used to define skin damage geometry, namely: size (average diameter), area, and depth (see Fig. 10). In the case of interleaved core sandwiches, all of these were found to increase continuously with impact energy and energy loss. Figures 14 and 15 show the effect of these variables on damage area and depth which may be representative for the overall damage geometry. It may be concluded from these relationships that the impact energy variable, and especially its energy loss component, have a direct, almost proportional, effect on damage area and depth. The effect of impact velocity and deceleration were less at low levels but become much more pronounced at the higher range. Damage size did not generally exceed the diameter of impactor tip.

Ultimate Failure and Residual Strength of Damaged Specimens Loaded in Flexure

In most cases of interleaved core sandwiches, ultimate failure was due to skin damage. Such failure was found to be a complex combination of three modes (see Fig. 16), namely, in-plane shear fracture along 30°, sublaminar delamination and buckling, and interlaminar separations between the CFRP laminate and GFRP fabric interleaf and external layers. Failure seems to originate always from the impact damage site. With few exceptions, premature shear core failure was the predominant mode (see Fig. 16). This was also the prevalent failure mode for the plain core sandwich version. Residual strength was determined by the value of skin compressive stress at sandwich failure (SSSF) which was computed by the approximate formulation given in Fig. 9. The

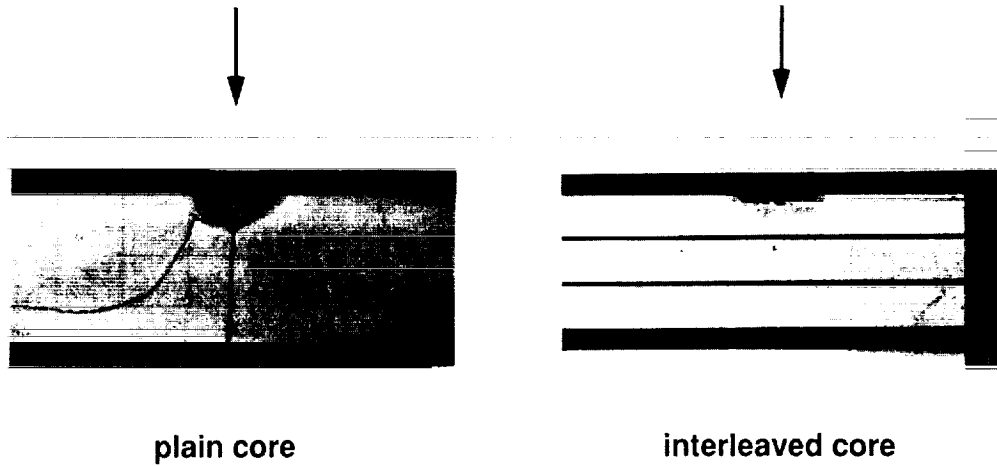


FIG. 12—Comparison of impact damage for interleaved versus plain foam core composite sandwiches, cross-sectional view (impact energy: 68.7 J).

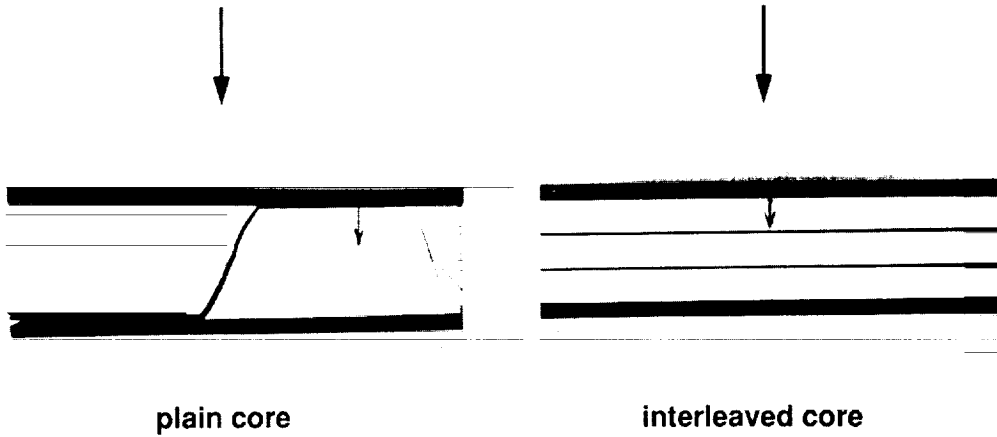


FIG. 13—Comparison of impact damage for interleaved versus plain foam core composite sandwiches, side view (impact energy: 68.7 J).

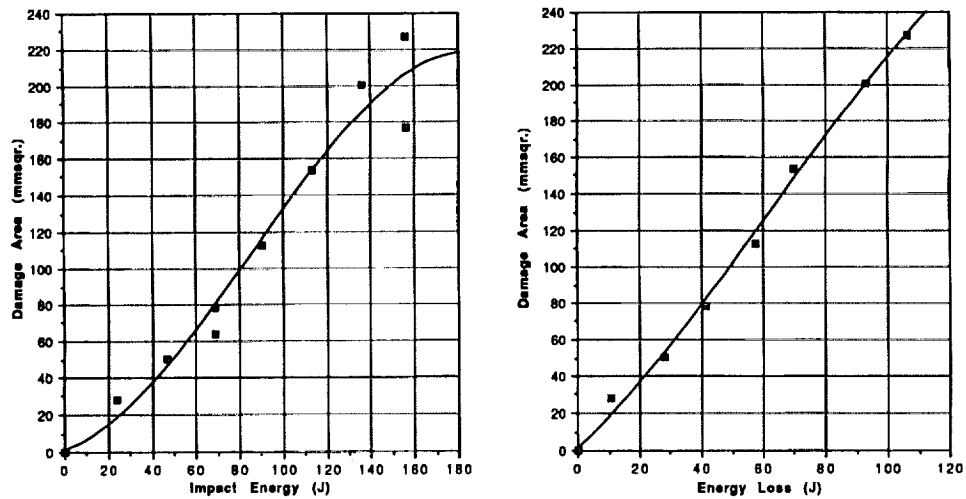


FIG. 14—The effect of low velocity impact energy and energy loss on damage area.

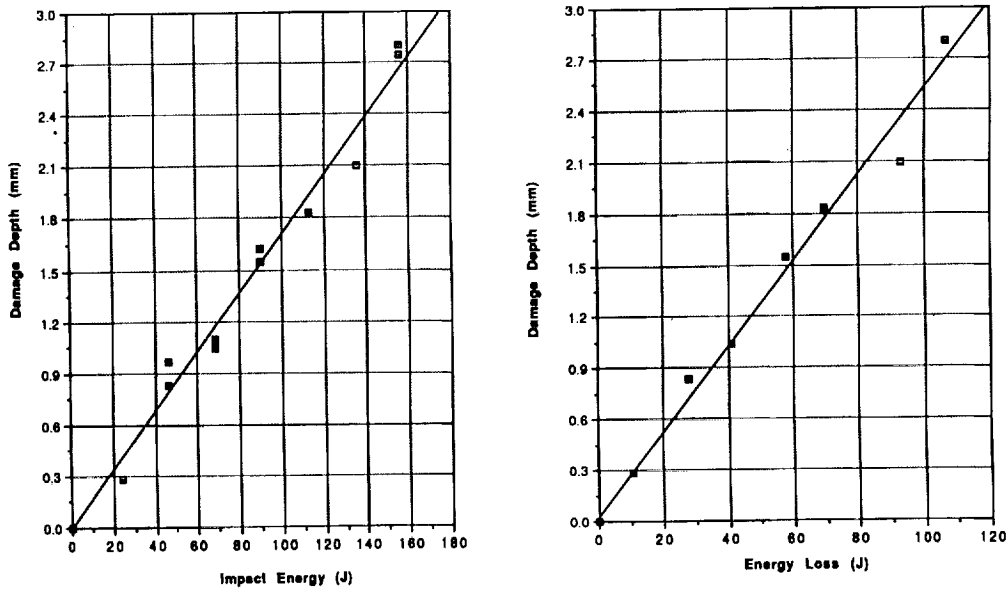


FIG. 15—The effect of low velocity impact energy and energy loss on damage depth.

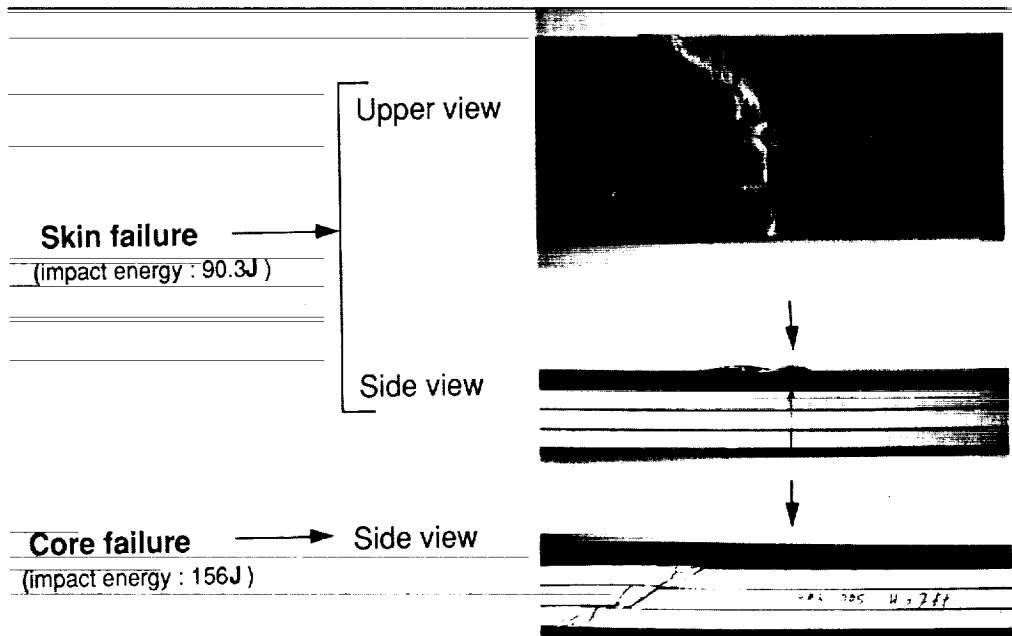


FIG. 16—Typical failure modes in residual strength test.

effects of damage characteristics and impact energy on SSSF for interleaved sandwich specimens damaged under low velocity impact are shown in Figs. 17 and 18. The trend common for all these relationships is the high rate of residual strength reduction at low impact values and the tendency to level off at the upper impact range. Residual strength levels of interleaved sandwich specimens that failed by core cracking are close to those obtained for cases of skin failure (Fig. 18).

Evaluation of Experimental Findings

Three main topics are dealt with in the present study, namely: the effect of interleaving, the comparison between low and high impact velocity, and mainly, the dependence of residual strength on damage and impact variables. The significant beneficial effect of interleaving on improving residual strength is clearly demonstrated in Fig. 19. The limited and scattered data for the plain

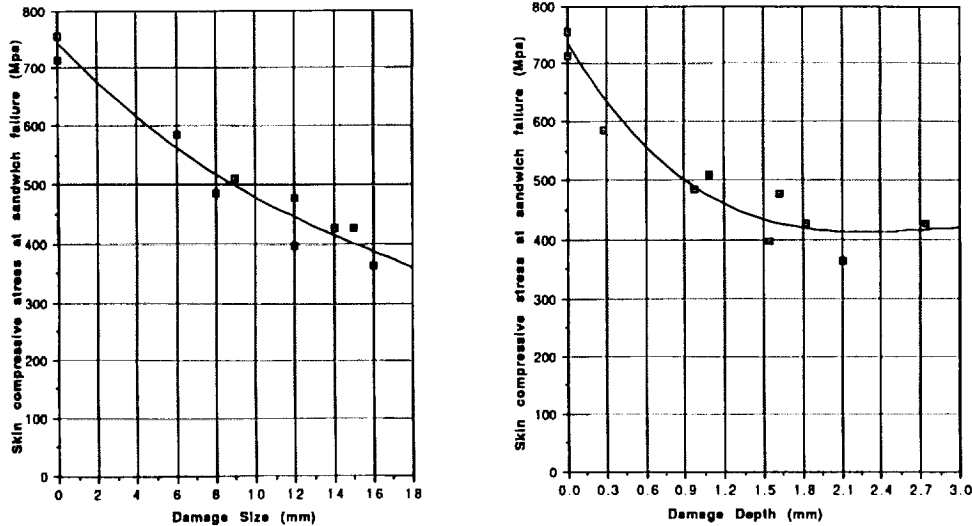


FIG. 17—The effects of damage size and depth on residual compressive strength of sandwich skin for interleaved core specimens subjected to low velocity impact.

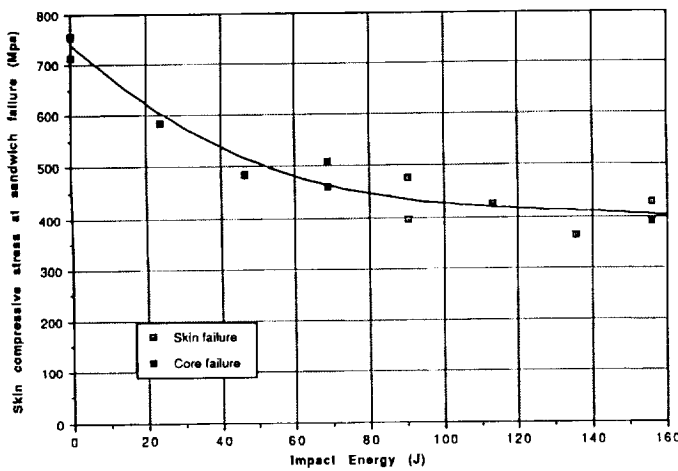


FIG. 18—The effect of impact energy on residual strength of sandwich panels with interleaved core subjected to low velocity impact.

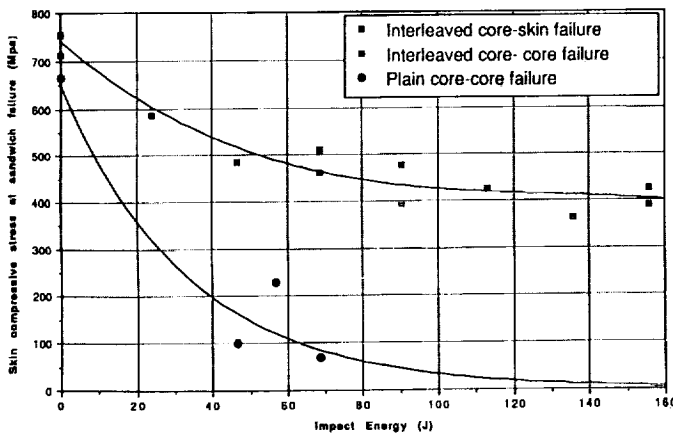


FIG. 19—The effect of low velocity impact energy on residual strength of sandwich panels (with plain versus interleaved foam core).

core sandwich specimens was due to premature cracking in the core which was not only caused by low impact energy but also by residual curing stresses as well. In most such cases, the disintegrated core could not support the skins and was unable to transfer stresses. Consequently, the sandwich had a very low stiffness and residual strength that did not reflect the structural potential of the CFRP skin. The interleaved core specimens, on the other hand, retained the expected residual strength and stiffness of the damaged skin even in cases of core failure. More than 50% of the original strength was retained at the higher level of impact energy applied at low velocity impact range (155 J).

Comparing the effect of impact velocity on residual strength as derived from drop-weight and ballistic tests (Fig. 20) revealed similar trends in spite of the large order of magnitude (≈ 25) difference in velocity between the two tests. This finding indicates that impact energy rather than velocity seems to be the prevailing variable that affects damage and residual strength. This premise is supported by plotting the data of residual strength versus impact energy derived from both low and high impact velocity tests on the same coordinates as shown in Fig. 21. Both sets of data are well intermingled within a single curve fit in spite of the fact that they were derived at widely different range of velocities and impactor weights. One of the main concerns in maintaining a damage-sensitive structural element is the ability to detect the occurrence, location, and size of an impact event. This information is needed for the decision whether to ignore, repair, or replace the damaged element, based mainly on evaluation of residual strength. An appropriate tool for this prediction is the "open hole model" as was demonstrated in Ref 26. The circular shape of the impact damage found in the present investigation justifies the use of the analytical solution of this model as formulated in Ref 43. The experimental data of residual strength versus normalized damage size for low velocity and ballistic impact tests is plotted and compared with the analytical prediction from Refs 43 and 44 (see Fig. 22). A full description of the analytical formulation for the present case is given in Ref 45. Good agreement between experiment and analysis for sizes up to the diameter of the impactor is evident. Note that the ana-

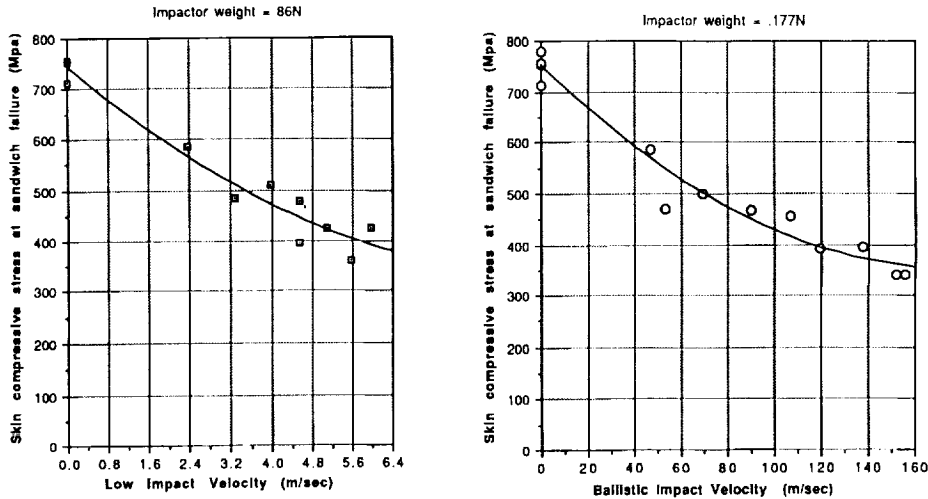


FIG. 20—The effect of impact velocity on residual compressive strength of sandwich skin (low velocity versus ballistic impact tests).

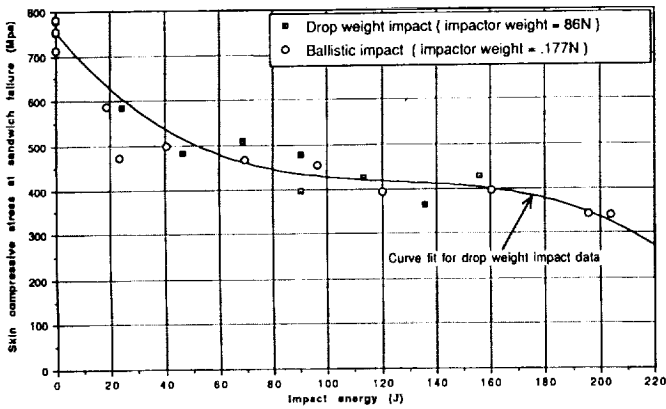


FIG. 21—The effect of impact energy on residual strength of sandwich panels with interleaved cores.

lytical model is for a plate of infinite width, whereas the present element is a finite-strip skin supported by a core. In spite of these reservations, it appears that the analytical prediction is valid for damage sizes smaller than one fourth of the sandwich width.

Conclusions

Based on the experimental results and their evaluation, the following conclusions may be drawn relating mainly to the damage tolerance performance of a composite sandwich system with an interleaved syntactic foam core suitable for elevated temperature applications.

- Damage tolerance performance is significantly improved by core interleaving.
- Impact failure is controlled by local skin damage, which can be inspected visually.

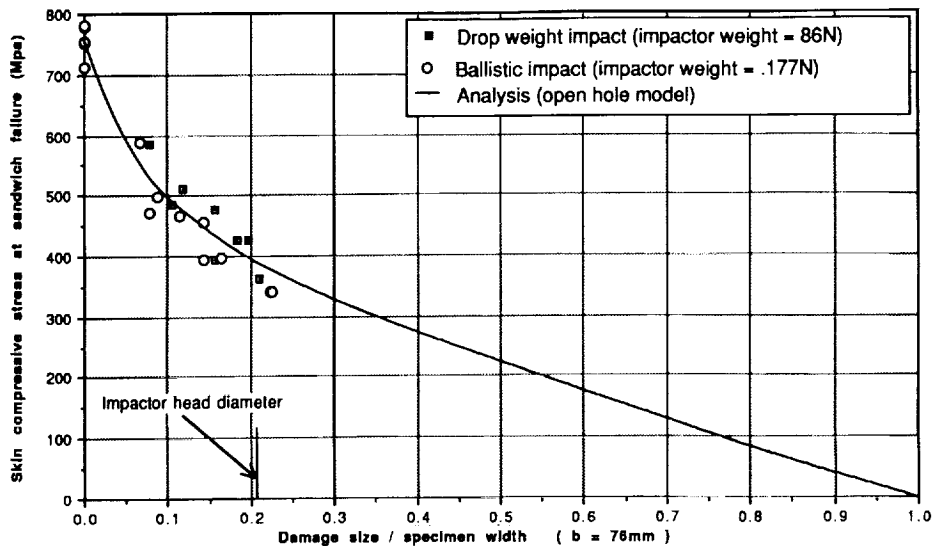


FIG. 22—The effect of normalized damage size on residual compressive strength of sandwich skin (low velocity and ballistic impact test results versus analytical solution).

- Residual strength decreases with impact energy down to about 50% of the original (at an energy level of 160 J).
- Damage and residual strength are directly dependent on impact energy rather than impact velocity or impactor weight.
- Damage size and residual strength are affected in the same way by both low velocity and ballistic impact energy.
- Residual strength may be predicted by visual measurements of damage size.

Acknowledgment

The authors wish to thank Dr. Howard Nelson, Roy Hampton, and Dave Chappell of the Test Engineering and Analysis Branch at NASA Ames Research Center for their support and encouragement and to Paul Scharmen of the Model Shop at the Center for the high-level manufacturing of the sandwich specimens.

References

- [1] Demuts, E., "Damage Tolerance of Composites," in *Proceedings of the American Society for Composites, 4th Technical Conference*, 1990, pp. 425-433.
- [2] Papoff, A. J., Dill, H. D., Sanger, K. B., and Kautz, E. F., "Certification of Damage Tolerance Composite Structures," in *Proceedings of 8th DOD/NASA/FAA Conference on Fibrous Composites in Structural Design*, 1989, pp. 499-514.
- [3] "Standard Tests for Toughened Resin Composites," NASA Reference Publication 1092, revised edition, 1983, 32 pp.
- [4] "Boeing Specification Support Standard: Advanced Composite Compression Test," BSS 7260, revised edition, 1986, 21 pp.
- [5] Falabella, R., Olsen, K. A., and Boyle, M. A., "Variations in Impact Test Methods for Tough Composites," in *Proceedings of 35th International SAMPE Symposium*, 1990, pp. 1454-1465.
- [6] Moon D. and Shivel, J. H., "Toward a Unified Method of Causing Impact Damage in Thick Laminated Composites," in *Proceedings of the 35th International SAMPE Symposium*, 1990, pp. 1466-1478.
- [7] Chen, C. H., Chen, M. Y., and Chen, J. P., "The Residual Shear Strength and Compressive Strength of C/E Composite Sandwich Structure After Low Velocity Impact," in *Proceedings of the 36th International SAMPE Symposium*, April 1991, pp. 932-943.
- [8] Starnes, J. H. and Williams, J. G., "Failure Characteristics of Graphite-Epoxy Structural Components Loaded in Compression," NASA Technical Memorandum 84552, 1982, 24 pp.
- [9] Cantwell, W. J. and Morton, J., "Comparison of the Low and High Velocity Impact Response of CFRP," *Composites*, Vol. 20, No. 6, 1989, pp. 545-551.
- [10] Zec, R. H., Wang, C. J., Mount, W. A., Jang, B. Z., and Hsieh, C. Y., "Ballistic Response of Polymer Composites," *Polymer Composites*, Vol. 12, No. 3, 1991, pp. 196-202.
- [11] Williams, J. G., O'Brien, T. K., and Chapman A. J., III, "Comparison of Toughened Composite Laminates Using NASA Standard Damage Tolerance Tests," NASA CP-2321, presented at ACEE Composite Structures Technology Conference, Aug. 1984, 72 pp.
- [12] Dempsy, R. L. and Horton, R. E., "Damage Tolerance Evaluation of Several Elevated Temperature Graphite Composite Materials," in *Proceedings of 35th International SAMPE Symposium*, 1990, pp. 1292-1305.
- [13] Ishai, O. and Shragai, A., "Effect of Impact Loading on Damage and Residual Compressive Strength of CFRP Laminated Beams," *Composite Structures*, Vol. 14, 1990, pp. 319-337.
- [14] Minguet, P., Dugudji, J., and Legace, A. P., "Buckling and Failure of Sandwich Plates with Graphite-Epoxy Faces and Various Cores," in *Proceedings of 28th Structures, Structural Dynamics and Materials Conference*, 1987, pp. 394-401.
- [15] Zenkert, D., "Strength of Sandwich Beams with Mid-Plane Debonding in the Core," *Composite Structures*, Vol. 15, 1990, pp. 279-299.
- [16] Zenkert, D., "Strength of Sandwich Beam with Interfacing Debonding," *Composite Structures*, Vol. 15, 1991, pp. 311-350.
- [17] Bass, M., Gottesman, T., and Fingerhut, U., "Criticality of Delamination in Composite Materials Structures," in *Proceedings of 28th Israel Annual Conference of Aviation and Astronautics*, 1986, pp. 186-190.
- [18] Ishai, O. and Rosenzweig, A., "The Effect of Interlaminar Flaw Characteristics on Residual Compressive Performance of GFRP Sandwich Specimens," *Annual Report on Damage Tolerance of Composite Materials*, Technion R&D Foundation Contract 893/9748/3-101, May 1990, Chap. 2, pp. 21-37.
- [19] Kassapoglou, C., "Buckling, Post-Buckling and Failure of Elliptical Delaminations in Laminate under Compression," *Composite Structures*, Vol. 9, 1988, pp. 135-159.
- [20] Sommers, M., Weller, T., and Abramovich, H., "Influence of Predetermined Delaminations on Buckling Behavior of Composite Sandwich Beams," *Composite Structures*, Vol. 17, 1991, pp. 292-329.
- [21] Gottesman, T., Bass, M., and Samuel, A., "Criticality of Impact Damage in Composite Sandwich Structure," in *6th International Conference of Composite Materials*, Vol. 3, 1988, pp. 327-335.
- [22] Steinman, A. E., "Damage Tolerance of Thin Skin Sandwich Panels," Report DFML-TR-76, Airforce Materials Laboratory, Wright-Patterson AFB, OH, Feb. 1977.
- [23] Farelly, G. L., "Effect of Low Velocity and Ballistic Impact Damage on the Strength of Thin Composite and Aluminum Shear Panels," NASA Technical Paper 2441, May 1985.
- [24] Rhodes, M. D., "Impact Fracture of Composite Sandwich Structure," NASA Technical Paper 75-718, 1975.
- [25] Thart, W. G. and Wanhill, R. J., "Impact Damage Effects on Fatigue of Composite Materials," NASA Report NLR-MP-82011-U, 1982.
- [26] Williams, J. G., "Effect of Impact Damage and Open Holes on the Compression Strength of Tough Resin/High Strain Fiber Laminates," in *NASA Conference Publication 2334, Proceedings of a Workshop Sponsored by NASA Langley Research Center*, May 1983, pp. 61-79.
- [27] Nettles, A. T., Lance, D. G., and Hodge, A. J., "A Damage Tolerance Comparison of 7075-T6 Aluminum Alloy and IM7/977-2 Carbon/Epoxy," in *Proceedings of the 36th International SAMPE Symposium*, April 1991, pp. 924-931.
- [28] Akay, M. and Hanna, R., "A Comparison of Honey-Comb Core and Foam Core Carbon Fiber-Epoxy Sandwich Panels," *Composites*, Vol. 21, No. 4, 1990, pp. 325-333.
- [29] Verpoest, I., Wevers, M., Ivens, J., and De Meester, P., "3D-Fabric for Compression and Impact Resistant Composite Sandwich Structures," in *Proceedings of 35th International SAMPE Symposium*, April 1990, pp. 296-307.
- [30] Nettles, A. T. and Hodge, A. T., "Impact Testing of Glass-Phenolic Honey-Comb panels with Graphite-Epoxy Face Sheets," in *Proceedings of 35th International SAMPE Symposium*, April 1990, pp. 1430-1440.
- [31] Lee, L. J., Huang, K. Y., and Fan, Y. J., "Dynamic Response of Composite Sandwich Plate Subjected to Low Velocity Impact," in *Proceedings of the Eight International Conference of Composite Materials*, July 1991, Paper 32-D.
- [32] Kan, H. P., Whitehead, S., and Kautz, E., "Damage Tolerance Certification Methodology for Composite Structures," in *NASA Conference Publication 3087, 8th DOD/NASA/FAA Conference on Fibrous Composites in Structural Design*, Nov. 1989, pp. 479-498.
- [33] Wong, R. and Abbott, R., "Durability and Damage Tolerance of Graphite-Epoxy Honey-Comb Structures," in *Proceedings of 35th International SAMPE Symposium*, April 1990, pp. 366-380.
- [34] Sela, N. and Ishai, O., "Interlaminar Fracture Toughness and Toughening of Laminated Composite Materials: a Review," *Composites*, Vol. 20, No. 5, 1989, pp. 423-435.
- [35] Altus, E. and Ishai, O., "The Effect of Soft Interleaved Layers on Combined Transverse Cracking-Delamination Mechanism in Composite Laminates," *Composite Science and Technology*, Vol. 39, 1990, pp. 13-27.
- [36] Sun, T. C. and Rechak, S., "Effect of Adhesive Layers on Impact Damage in Composite Laminates," in *Composite Materials: Testing and Design (Eighth Conference)*, ASTM STP 972, J. D. Whitcomb, Ed., American Society for Testing and Materials, Philadelphia, 1988, pp. 97-123.
- [37] Sun, T. C. and Norman, T. L., "Design of a Laminated Composite with Controlled-Damage Concept," *Composite Science and Technology*, Vol. 39, 1990, pp. 327-340.
- [38] Frazier, J. L. and Clemons, A., "Evaluation of Thermoplastic Film Interleaf Concept for Improved Damage Tolerance," in *Proceedings*

- of 35th International SAMPE Symposium, April 1990, pp. 1620-1627.
- [39] Jang, B. Z., Chen, L. C., Wang, C. Z., Lin, H. T., and Zee, R. H., "Impact Resistance and Energy Absorption Mechanism in Hybrid Composites," *Composite Science and Technology*, Vol. 34, 1989, pp. 305-335.
- [40] Wang, C. J. and Jang, B. Z., "Impact Performance of Polymer Composites: Deformation Process and Fracture Mechanisms," in *Proceedings of the Eighth International Conference of Composite Materials*, Paper 32-B, 1991.
- [41] Busgen, A. W., Effing, M., and Scholle, M., "Improved Damage Tolerance of Carbon Fibre Composite by Hybridization with Polyethylene Fibre, Dyneema SK 60," in *Proceedings of 4th Technical Conference of the American Society for Composites*, 1989, pp. 418-424.
- [42] Avery, J., Allen, M. R., Sawdy, D., and Avery, S., "Survivability Characteristics of Composite Compression Structure," *NASA Conference Publication 3087, Proceedings of 8th DOD/NASA/FAA Conference on Fibrous Composites in Structural Design*, 1989, pp. 455-478.
- [43] Whitney, J. M. and Nuismer, R. J., "Stress Fracture Criteria for Laminated Composites Containing Stress Concentrations," *Journal of Composite Materials*, Vol. 8, July 1974, pp. 253-265.
- [44] Nuismer, R. J. and Labor, J. D., "Application of the Average Stress Failure Criterion: Part II-Compression," *Journal of Composite Materials*, Vol. 13, Jan. 1979, pp. 49-60.
- [45] Hiel, C. and Ishai, O., "Low and High Velocity Impact Response of Sandwich Panels with Syntactic Foam Core," in *Proceedings of the ASME Symposium on Recent Advances in Structural Mechanics*, PVP Vol. 225/NE-Vol. 7, Dec. 1991, pp. 137-141.

Designer's Corner

Short contributions of less than 1000 words plus key illustrations are being invited, covering topical issues associated with the design and application of composites. Notable designers from a broad range of industries including aerospace, automotive, civil, bioengineering and recreational are encouraged to submit a contribution to this section. Communications may cover, but not necessarily be restricted to, the following subjects:

- novel and innovative concepts in composites design and fabrication;
- economics issues and other impediments to the wider exploitation of composites;

- selection approaches for the various available fibre architectures and processes;
- choice of failure criteria used for establishing integrity of composite products;
- effective concurrent engineering approaches.

Contributions will be subject to a rapid review and publication process. Prospective contributions, marked for the 'Designer's Corner', should be submitted to: Dr Keith T. Kedward, Department of Mechanical & Environmental Engineering, University of California, Santa Barbara, CA 93106, USA. Fax: 1 (805) 893 8651

Composite sandwich construction with syntactic foam core

A practical assessment of post-impact damage and residual strength

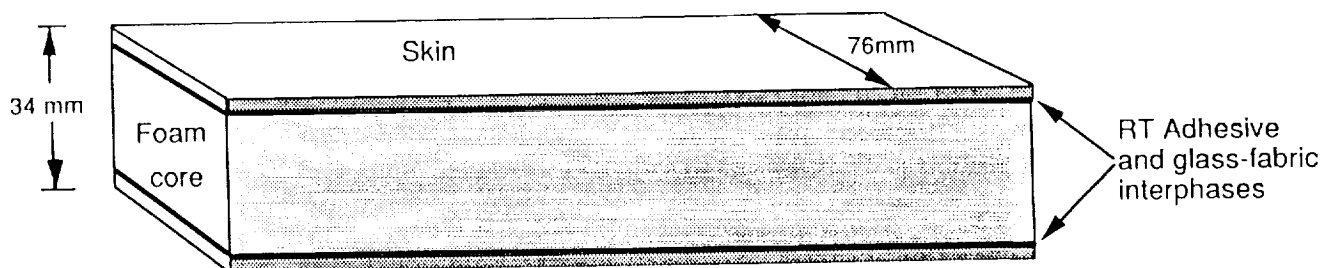
C. HIEL, D. DITTMAN and O. ISHAI

(NASA Ames Research Center, USA)

Most composite sandwich constructions with a light-weight core are difficult to reliably inspect for post-impact damage. Additionally the residual strength cannot easily be estimated, and therefore aeronautical

designers tend to prefer a skin-stringer type arrangement for primary load-bearing structures.

The purpose of this note is to report on a successful



Skins composition : CFRP - Rigidite 5245C/G40-600 **Lay-up :** (0/+30/-30)_{3s}
+ GFRP Fabric - 7781-5245C - 2 external layers (for surface protection)

Core composition : Syntactic foam - Syntac 350 (glass micro balloons in epoxy resin)

Interphases composition : Hysol EA9394 Adhesive + GFRP Fabric

Fig. 1 Sandwich configuration with syntactic foam core

inspection method for sandwich panels with syntactic foam core and to summarize a procedure for the practical assessment of post-impact damage and residual strength.

A syntactic foam core is a composite itself, since it often contains 50% (by weight) of hollow glass or ceramic microspheres in a thermoset matrix. A disadvantage is that its weight is typically four to eight times higher than that of the traditional foams used in aerospace applications. One main advantage is that the mechanical properties of syntactic foams are several orders of magnitude higher than those of the lighter (traditional) foams¹. Sandwich construction with syntactic foam core therefore provides a sensible approach for land- or marine-based applications, where damage tolerance and residual strength, rather than weight savings, dominate the design requirements.

After a feasibility study conducted at NASA Ames Research Center, the concept shown in Fig. 1 was selected as the basis for the design of highly damage-tolerant composite wind tunnel compressor blades. Hybrid glass fibre-reinforced plastic/carbon fibre-reinforced plastic (GFRP/CFRP) composite skins were bonded onto a syntactic foam core. Details of the materials together with manufacturing and test procedures are given elsewhere^{1,2}.

Extensive low- and high-velocity impact tests revealed that the damage was always localized and confined. This confinement, as shown in Fig. 2, is due to the energy-absorbing capacity of the glass microspheres which are part of the syntactic foam core. Additionally, as shown in Fig. 3, the imprint formed at the GFRP external surface is localized and clearly visible to the unaided eye. This visibility is due to local delamination, over an area which is slightly elliptical (with major axis D), at the hybrid GFRP/CFRP skin interface and has a practical significance, as is demonstrated below.

This technical note will address two specific issues: First, what makes this sandwich system damage tolerant? Second, how can the residual compressive strength after impact be determined?

Analytical models to predict the residual strength of open-hole composite samples as a function of hole size are available in several publications³⁻⁵. Fig. 4(a) shows an impact-damaged skin and Fig. 4(b) shows a skin in which a hole of diameter D was drilled. The residual strengths of both specimens were found to be equivalent for D ranging between 10 and 20 mm. This in turn suggests that the imprints on the GFRP skin coating are a replica of the damage; hence, a measure of the imprint size will allow the prediction of the residual strength of an impact-damaged sandwich.

The localized and confined nature of the impact damage is attributed to the high energy-absorption capacity of the syntactic foam. Scanning electron microscopy (SEM) reveals that most of the impact energy is consumed through crushing of the glass microspheres. This failure mechanism reigns within a hemispherical zone, which is centred at the point of impact and spreads downwards into the syntactic foam core material. This zone is defined by the discolouration of the core, as shown in Fig. 2, which is evidently due to the failed microspheres.

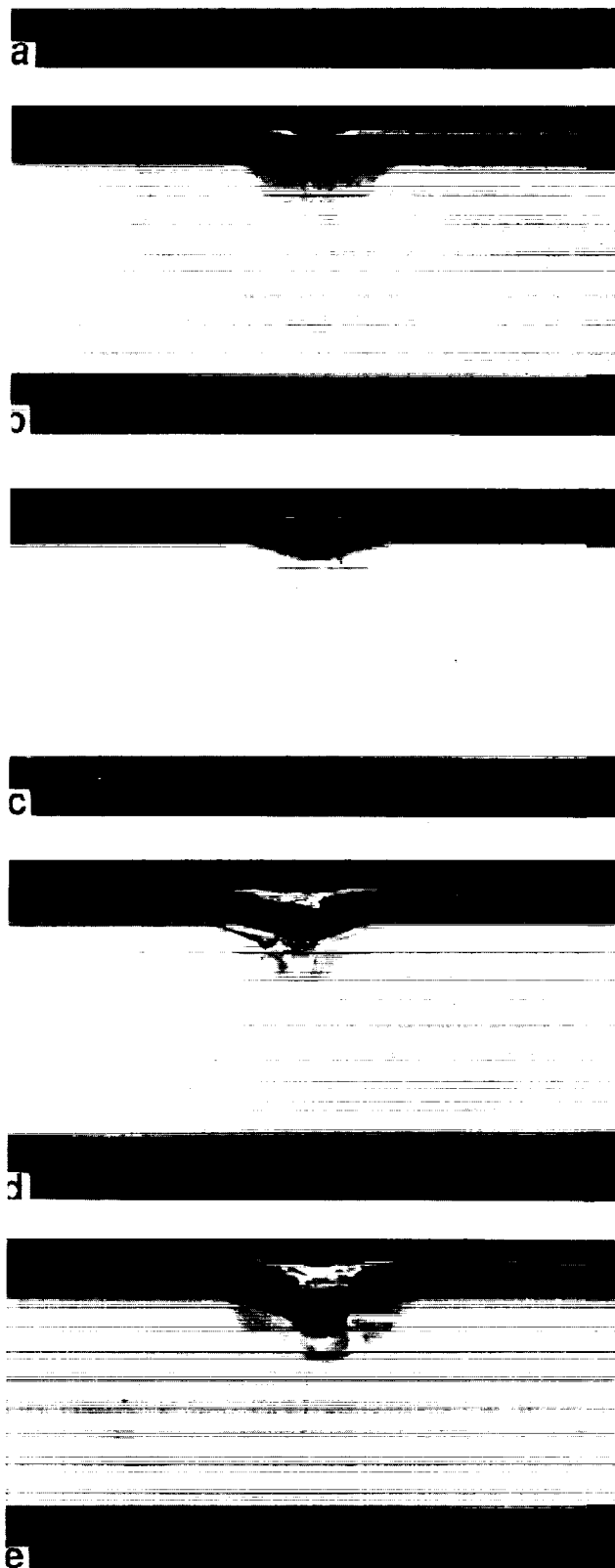


Fig. 2 Confined damage after low-velocity impact at impact energy levels of: (a) 47 J; (b) 69 J; (c) 90 J; (d) 136 J; (e) 180 J

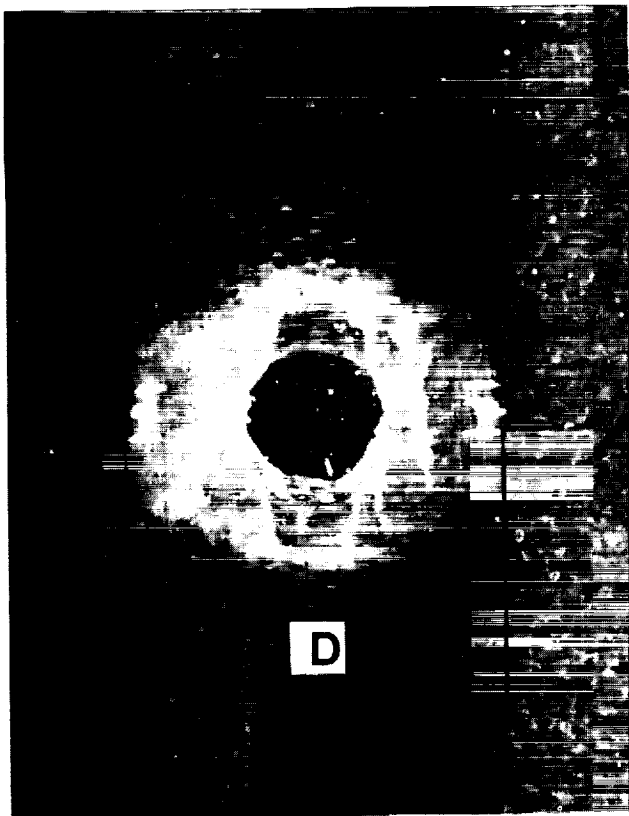


Fig. 3 Damage imprint at the external GFRP surface

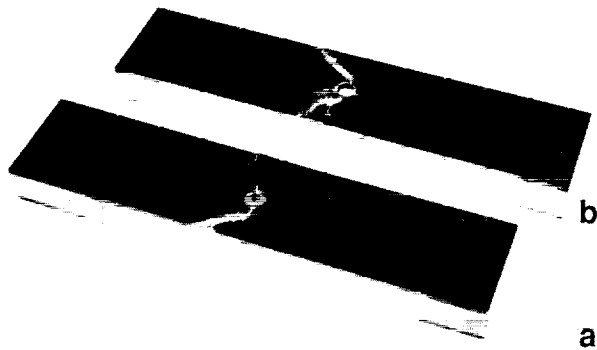


Fig. 4 Comparison of sandwich skins with impact damage and open hole

This is seen from the enlarged micrograph of Fig. 5(a), which was taken inside the discoloured zone, in contrast to Fig. 5(b) which was taken outside this zone.

SEM was also used to observe the microstructural pattern of the impact damage. Micrographs of cross-sections in Fig. 6 show the damage for five (low-velocity) impact energy levels. The CFRP skin damage zone can be clearly observed and compared with the GFRP imprint size and the core damage size. Results of these measurements are shown in Fig. 7. A good correlation between external (GFRP) imprint size and internal (CFRP) damage size is

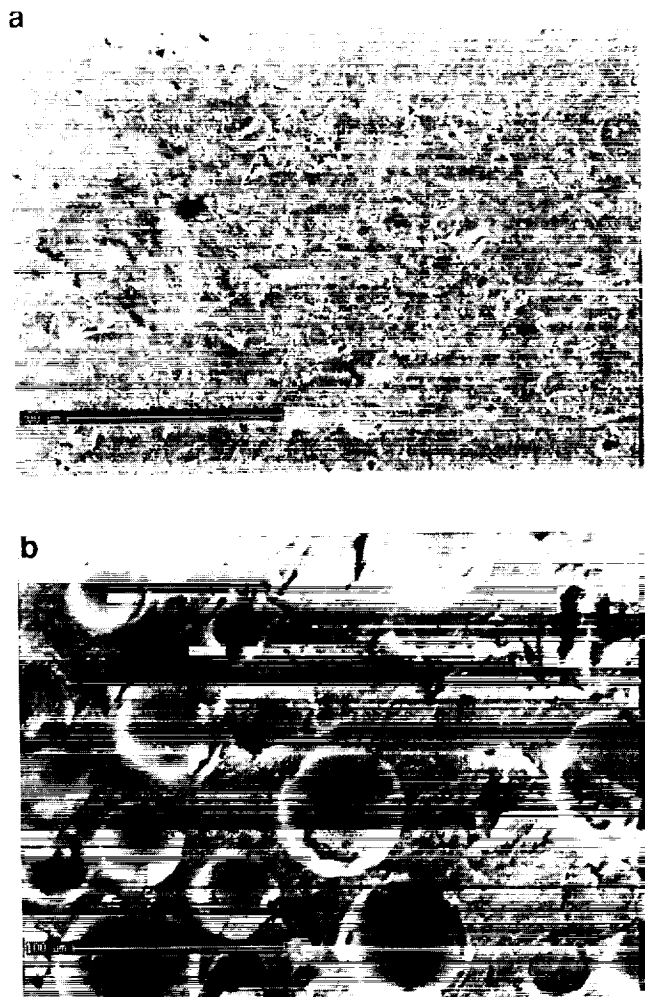


Fig. 5 SEM micrographs taken (a) inside discoloured zone and (b) outside discoloured zone

evident whereas the core damage size (defined by the extent of discolouration) is consistently larger.

Thus highly damage-tolerant sandwich constructions can be obtained by using hybrid composite skins and a syntactic foam core. This is achieved by localization of the damage due to the high absorption of impact energy via crushing of the glass microballoons. The local region of skin failure may be represented by an external imprint that is clearly visible to the unaided eye. Post-impact strength can be predicted by direct measurement of the imprint size using available open-hole theories.

The concept which was suggested for the design of highly damage-tolerant wind tunnel compressor blades combines three material phases with specific purposes:

- 1) CFRP skins, which are the structural backbone, to provide high specific strength and stiffness;
- 2) syntactic foam core which has high mechanical properties and therefore provides an excellent shear tie between the skins. Additionally it supports the skins against buckling, localizes the impact damage and absorbs energy through a microballoon crushing mechanism; and
- 3) GFRP fabric which acts as a sacrificial protective coating for the CFRP and serves as a visual enhancement of impact damage for residual strength assessment.

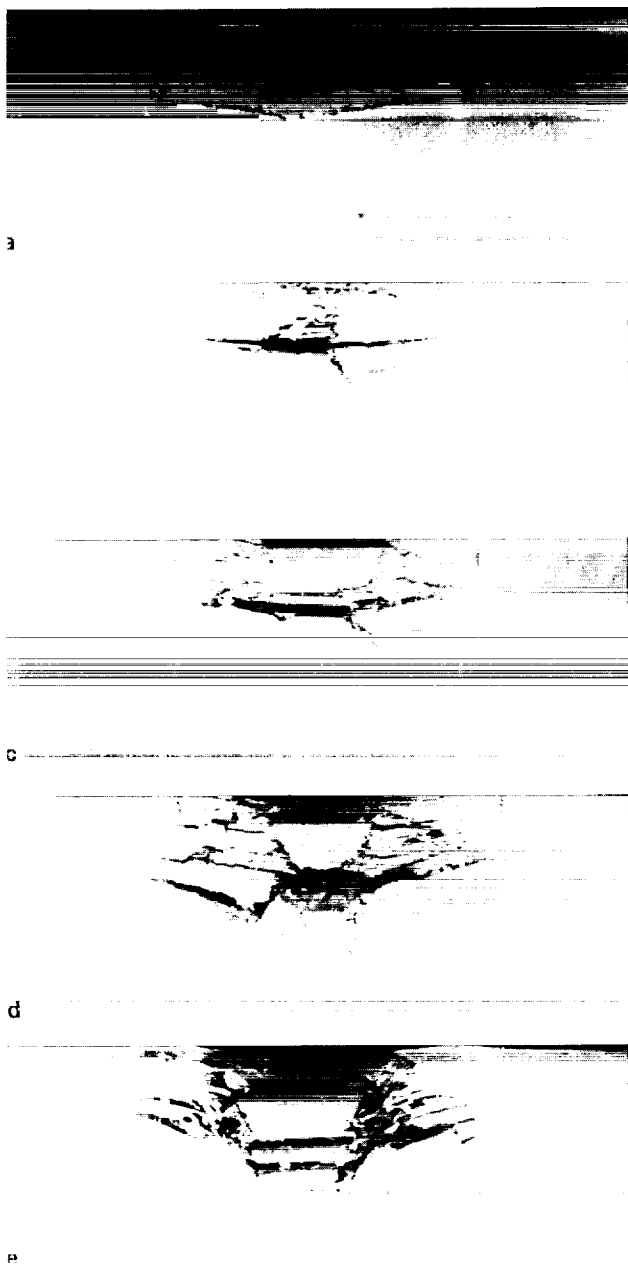


Fig. 6 SEM micrographs of localized damage for five (low-velocity) impact energy levels: (a) 47 J; (b) 69 J; (c) 90 J; (d) 136 J; (e) 180 J

The design with syntactic foam may be appropriate for many applications where the design is driven by damage tolerance rather than by weight. The findings presented here indicate that concepts and design notions valid for

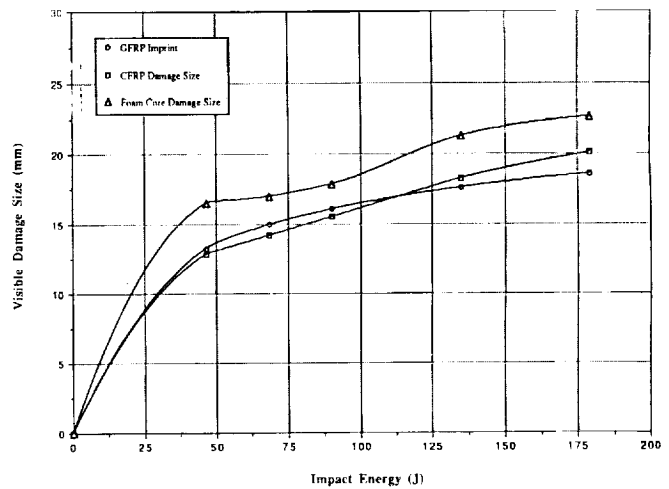


Fig. 7 Effect of low-velocity impact energy on damage size in GFRP, CFRP and foam core

aerospace-type constructions need to be modified when transferring technology to a land-based application.

REFERENCES

- 1 Hiel, C. and Ishai, O. 'Design of highly damage-tolerant sandwich panels' *37th Int SAMPE Symp. March 1992* pp 1228-1242
- 2 Ishai, O. and Hiel, C. 'Damage tolerance of a composite sandwich with interleaved foam core' *J Composite Technol Res* **14** No 3 (Fall 1992) pp 155-168
- 3 Whitney, J.M. and Nuismer, R.J. 'Stress fracture criteria for laminated composites containing stress concentrations' *J Composite Mater* **8** (July 1974) pp 253-265
- 4 Nuismer, R.J. and Labor, J.D. 'Application of the average stress failure criterion: Part II - Compression' *J Composite Mater* **13** (January 1979) pp 49-60
- 5 Hiel, C. and Ishai, O. 'Effect of impact damage and open hole on compressive strength of hybrid composite skin laminates' *ASTM Symp on Compression Response of Composite Structures, 16-17 November 1992*

AUTHORS

Dr Clement Hiel, to whom correspondence should be addressed, is a Principal Investigator with the Composite Materials R&D Program, EEM Branch, NASA Ames Research Center, Moffett Field, CA 94035, USA. Dan Dittman is a Research Engineer, specializing in materials failure analysis, and Dr Ori Ishai is a Visiting Scientist, specializing in mechanics of composite materials, at EEM Branch, NASA Ames Research Center. Permanently, Dr Ishai a Professor at Technion, Israel Institute of Technology, Haifa, Israel.